Annales Henri Lebesgue
7 (2024) 787-821

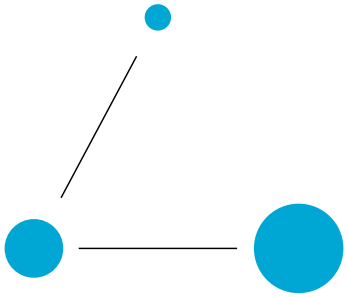

ANNALES
HENRI LEBESGUE

JULIEN BOULANGER
ERWAN LANNEAU
DANIEL MASSART

ALGEBRAIC INTERSECTION FOR A FAMILY OF VEECH SURFACES

INTERSECTION ALGÉBRIQUE POUR UNE FAMILLE DE SURFACES DE VEECH

Abstract. — We study some properties of the function KVol defined by

$$\mathrm{KVol}(X,\omega) := \mathrm{Vol}(X,\omega) \sup_{\alpha,\beta} \frac{\mathrm{Int}(\alpha,\beta)}{l_g(\alpha) l_g(\beta)}$$

on the moduli space of translation surfaces. For the Teichmüller discs $\mathcal{T}_n$ of the original Veech surfaces arising from the right-angled triangles $(\pi/2, \pi/n, (n-2)\pi/2n)$ for odd $n \geqslant 5$, we establish the first known explicit formula for KVol (beyond the case of the moduli space of flat tori).

Résumé. — On étudie la fonction KVol sur les espaces de modules de surfaces de translation définie par

$$\mathrm{KVol}(X,\omega) := \mathrm{Vol}(X,\omega) \sup_{\alpha,\beta} \frac{\mathrm{Int}(\alpha,\beta)}{l_g(\alpha) l_g(\beta)}.$$

En particulier, sur les disques de Teichmüller $\mathcal{T}_n$ des surfaces de Veech associées au billard dans les triangles $(\pi/2, \pi/n, (n-2)\pi/2n)$ pour n impair $\geqslant 5$, nous donnons la première formule explicite connue pour KVol (en dehors du cas des espaces de modules de tores plats).

Keywords: Lyapunov exponents, translation surface, Teichmüller curve, algebraic intersection.
2020 *Mathematics Subject Classification:* 37E05, 37D40.
DOI: `https://doi.org/10.5802/ahl.211`
(*) This work has been partially supported by the LabEx PERSYVAL-Lab (ANR-11-LABX-0025-01) funded by the French program Investissement d'avenir.

1. Introduction

Our objects of study are translation surfaces and their geodesics. These structures arise in the study of rational polygonal billiards and more generally in Teichmüller dynamics. This paper focuses on computing relations between lengths of geodesics and their intersections on those surfaces.

1.1. Motivation and results

For any closed (meaning compact, connected, without boundary) oriented surface X, the algebraic intersection endows the first homology group $H_1(X,\mathbb{R})$ with a symplectic bilinear form denoted $\mathrm{Int}(\cdot,\cdot)$. When X is endowed with a Riemannian metric g (possibly with singularities), one can ask the following question: how much can two curves of a given length intersect? Namely, what is

$$\mathrm{KVol}(X) := \mathrm{Vol}(X,g)\cdot \sup_{\alpha,\beta} \frac{\mathrm{Int}(\alpha,\beta)}{l_g(\alpha) l_g(\beta)}, \tag{1.1}$$

where the supremum ranges over all piecewise smooth closed curves α and β in X, and $l_g(\cdot)$ denotes the length with respect to the Riemannian metric. It is readily seen that multiplying by the volume $\mathrm{Vol}(X,g)$ makes the quantity invariant by rescaling the metric g. This function is well defined, finite (see [MM14]) and continuous in the metric.

Recent work [CKM21a, CKM21b] provides estimates of KVol on Teichmüller curves of some square-tiled translation surfaces (X,ω). In this paper we shed some light into the case of non-square-tiled surfaces, namely we investigate the family of Veech surfaces [Vee89], obtained for odd $n \geqslant 5$ by gluing opposite sides of two copies of a regular n-gon. The associated Teichmüller curve $\mathcal{T}_n$ is canonically identified with $\mathbb{H}^2/\Gamma_n$, where Γ_n is the Hecke triangle group of signature $(2,n,\infty)$ (see Section 2 and Section 4). In this context, we establish the first known explicit formula for KVol (beyond the case of the moduli space of flat tori, see [MM14]).

THEOREM 1.1. — *For any odd integer $n \geqslant 5$, and any $(X,\omega) \in \mathcal{T}_n$,*

$$\mathrm{KVol}(X,\omega) = \frac{\frac{n}{2}\cot\frac{\pi}{n}\cdot\frac{1}{\sin\frac{\pi}{n}}}{\cosh d_{\mathrm{hyp}}(X,\gamma_{0,\infty})},$$

where $\gamma_{0,\infty}$ is the hyperbolic geodesic in $\mathbb{H}^2$ with endpoints 0 and ∞.

In particular KVol is real analytic on $\mathcal{T}_n$ except along the geodesic with endpoints $\cos\frac{\pi}{n}$ and ∞.

Remark 1.2. — The quantity KVol appears naturally in the comparisons between the stable norm $\|\cdot\|_s$ and the Hodge norm. More precisely (see [Mas96, MM14]):

$$\|\cdot\|_s \leqslant \sqrt{\mathrm{Vol(M,g)}}\,\|\cdot\|_{\mathrm{H}odge} \leqslant \mathrm{KVol}(M,g)\|\cdot\|_s$$

The upper bound is sharp. There is a nice interpretation of KVol, as the solution to a geometric optimisation problem: what is the largest area, with respect to the symplectic intersection form, of a parallelogram inscribed in the unit ball of the stable norm?

1.2. Context and history

While KVol is a close cousin of the systolic ratio $\sup_\alpha \frac{\mathrm{Vol}(X,g)}{l_g(\alpha)^2}$, very little is known on the function KVol. For any Riemannian surface (X, g), we have $\mathrm{KVol}(X, g) \geqslant 1$, and equality holds if and only if (X, g) is a flat torus [MM14]. Almost all of the obvious questions about KVol on hyperbolic surfaces are currently open.

In this paper we propose to continue the study of KVol as a function on the moduli space of translation surfaces, originally initiated by the third named author in [CKM21a, CKM21b]. Translation surfaces are rich objects that may be seen from many different angles. In our context, we will use the definition in terms of Euclidean polygons. Informally we will consider translation surfaces as objects constructed by gluing polygons along parallel sides of the same length using translations. More formally, if P is a (finite set of) Euclidean polygon(s), we say that h is a pairing of the edges $E(P)$ if every $e \in E(P)$ is mapped to $h(e)$ by a translation τ_e, such that τ_e sends the unit vector normal to e (pointing toward the interior of P) to the unit vector normal to $h(e)$ (pointing toward the exterior of P). After identifications of e with $\tau_e(e)$, we will say that the quotient X is a (possibly non connected) translation surface, with polygonal representation P and pairing h.

In this paper the polygons we will mainly consider are pairs of regular $n = 2m + 1$-gons, glued by one side, with "obvious" opposite sides identified, see Figure 2.1. The translation surface we obtain will be denoted by X_0 and will be referred to as the *double regular $n-$gon*.

A translation surface inherits the metric of the Euclidean plane everywhere but (possibly) at the images of the vertices of P (called the singularities). In particular, the geodesics may be viewed as straight lines, until they hit a singularity. Geodesic trajectories that start and end at a singularity (not necessarily the same) are referred to as *saddle connections*. In particular, although geodesics on X are piecewise straight lines, they can be quite complicated as they may be unions of saddle connections with different directions. In fact, every closed curve on a translation surface is homologous to a union of saddle connections, which can be chosen so as to minimize the length in its homology class.

Remark 1.3. — In this paper, as in [CKM21a], we get major help from the fact that the surface has only one singularity, so every saddle connection is closed. By a convexity argument, this means that in (1.1) we may take the supremum over pairs of saddle connections.

In [CKM21a], KVol is studied for ramified covers of the torus (or arithmetic Teichmüller curves). It is proved in [CKM21a] that KVol, defined on the Teichmüller curve of the surface tiled with three squares, is unbounded, but it does have a minimum, achieved at a surface, unique modulo symmetries, and otherwise fairly undistinguished. The interesting surfaces, i.e. the three square surfaces, and the surface tiled with six equilateral triangles, are local maxima, with $\mathrm{KVol} = 3$, where 3 should be thought of as the ratio of the total area of the surface, to the area of the smallest cylinder of closed geodesics. The local maxima are not locally unique, they come in hyperbolic geodesics, in the Teichmüller curve viewed as a quotient of the hyperbolic plane by a Fuchsian group.

1.3. KVol on non arithmetic Teichmüller curves

The fundamental ingredient for the study of the dynamics of the translation flow on a surface is the natural action of the group $\mathrm{GL}(2,\mathbb{R})$ on the moduli space of the set of all translation surfaces having the same genus (the action is given by the linear action on the polygons defining the translation surface). Since KVol is constant along any $\mathrm{SO}(2,\mathbb{R})$-orbit, we will naturally consider KVol as a function on the quotient

$$\mathcal{T} = \mathrm{SO}(2,\mathbb{R})\backslash \mathrm{SL}(2,\mathbb{R}) \cdot X = \mathbb{H}^2/\mathrm{Stab}(X)$$

(see Section 4 for details). Throughout this paper we restrict our attention to the case where $\mathcal{T}$ has finite volume, or equivalently $\mathrm{SL}(X) := \mathrm{Stab}(X)$ is a lattice in $\mathrm{SL}(2,\mathbb{R})$. We will say that X is a Veech surface. As discussed above, the simplest source of Teichmüller curves is the torus covers. From Theorem 1.1, we deduce the following more precise statement for the non-square-tiled surfaces obtained by Veech [Vee89].

Corollary 1.4. — *For odd integer $n \geqslant 5$, let $\mathcal{T}_n$ be the Teichmüller curve of the double regular $n-$gon. For any $X \in \mathcal{T}_n$ the following holds*

$$\frac{n}{2}\cot\frac{\pi}{n} \leqslant \mathrm{KVol}(X) \leqslant \frac{n}{2}\cot\frac{\pi}{n}\cdot\frac{1}{\sin\frac{\pi}{n}}.$$

Moreover the bounds are sharp and:

1. *The maximum of the function* KVol *on $\mathcal{T}_n$ is achieved, precisely, along $\gamma_{0,\infty}$, that is, by images of the right-angled staircases under the Teichmüller geodesic flow (see Figure 2.1).*
2. *The minimum of the function* KVol *on $\mathcal{T}_n$ is achieved, uniquely, at X_0.*

Finally, in the definition of KVol*, the supremum is achieved by pairs of curves that are (images of) pairs of sides of the double regular $n-$gon.*

Remark 1.5. — The case of the regular $4m$-gon, which is combinatorially more complicated, is dealt with in [Bou23a].

One of the reasons it is more complicated is that on the staircase model associated with the regular $4m$-gon KVol is both achieved as the ratio $\frac{\mathrm{Int}(\alpha,\beta)}{l(\alpha)l(\beta)}$ for a unique pair (α,β) and the limit of the same ratio for a family of pairs of closed curves, whereas on the staircase model associated with the double regular $2m+1$-gon the maximizing pair of curve wins by a large margin over any other pair of curves, and hence the same pair of curves maximizes KVol for small deformations of the staircase of the $2m+1$-gon. This is due to the shape of cylinder decompositions. Also, the analog of Proposition 6.1 is combinatorially more complicated and requires a more precise estimation of the length of some saddle connections.

Remark 1.6. — Another notable consequence of Theorem 1.1 is that the supremum in the definition of KVol, is actually a maximum, for every $X \in \mathcal{T}_n$. This is not a general fact about translation surfaces, not even about Veech surfaces, since it is not the case for almost every flat torus [MM14]. However we suspect it might be the case for Veech surfaces of genus larger than two, with the following heuristic argument. In a Veech surface, every direction is either completely periodic, or uniquely ergodic [Vee89]. This means that if the supremum in (1.1) is not achieved by closed

geodesics, it must be achieved, in a generalized sense, by a pair (α, β) where at least one of α, β is an irrational foliation instead of a closed curve. But irrational foliations, which are dense in a Veech surface, visit the whole surface, hence they take up too much length, for what little intersection you can get out of them, to be serious candidates to realize KVol.

Unlike the three-square surface case [CKM21a], KVol is bounded on the Teichmüller discs of the double regular $n-$gon. In fact this holds for other Veech surfaces than the double $n-$gon. Our second main result is the first step toward a classification of $\mathrm{GL}(2,\mathbb{R})$-orbits with bounded KVol.

THEOREM 1.7. — KVol *is bounded on the Teichmüller disc of a Veech surface having only one singularity if and only if there are no parallel saddle connections intersecting non trivially.*

The first author proved a more general version of Theorem 1.7, which applies to translation surfaces with several singularities, see [Bou23a, Bou23b]. As a corollary, we obtain

THEOREM 1.8. — *If X is a genus two surface with only one singularity, then the function* KVol *is bounded on the Teichmüller disc of X if and only if X is a primitive Veech surface i.e. X is not arithmetic.*

In fact, the same discussion applies to the Teichmüller disc of surfaces in the Prym eigenform loci in genus three and four (with one singularity, see [LN14]) by looking at possible cylinder diagrams.

Remark 1.9. — Another difference with [CKM21a] is that the minimum of KVol on $\mathcal{T}_n$ is achieved, uniquely, by the most interesting surface in the disc, namely the double $n-$gon. On the other hand, similarly to the three-square case, the local maxima, which are also global maxima, are achieved along hyperbolic geodesics in the Teichmüller disc, which correspond to surfaces with a right-angled template, see Figure 2.1.

1.4. Strategy for the proof of Theorem 1.1

One of the main reasons why KVol is complicated to compute is that the set of curves on a surface is hard to grasp. For translation surfaces, this is also the case: saddle connections can be very complicated. However saddle connections come in families, given by the $\mathrm{SL}(2,\mathbb{R})$-action. Remarkably, for Veech surfaces, as observed in [Vee89], directions of saddle connections correspond to the cusps of the corresponding Teichmüller curve. Even more specifically, in our situation, the double n-gons, the fundamental domains of the associated Veech groups have a simple shape, with only one cusp (see Figure 2.2) and simple identification patterns on the boundary. This also implies that all cylinder decompositions look the same up to the action of $SL(2,\mathbb{R})$. These reasons explain why the family of double n-gons is amenable to the computation of KVol.
We know briefly explain the main steps of the proof.

- We first compute KVol on the right angled staircases of the Teichmüller disks: for any (closed) saddle connection α, one decomposes the surface into cylinders in the direction of α. This gives a bound on the ratio $\mathrm{Int}(\alpha,\beta)/l(\alpha)l(\beta)$ for any saddle connection β, see Proposition 5.3. On the staircase model associated to the double regular n-gon, this bound is achieved (uniquely) by the pair of systoles, intersecting once (Remark 5.4). However, for surfaces in the Teichmüller disk that are not right angled, the bound is not attained, and we need to refine our interpretation of KVol: this is done in Section 4 and Section 5, and the main result is Proposition 5.1.
- Then, we compute KVol on the double regular n-gon. We use a completely different method: given two saddle connections α and β, we subdivide them into shorter (non-closed) segments for which we can control both the length and the number of intersection points. This is the content of Section 6.
- Finally, we relate the pairs of curves that achieve the supremum in the definition of KVol on the right angled staircases and the double regular n-gon using the action of $SL(2,\mathbb{R})$. This is done using the formalism of Section 4 and Section 5, and we show in Section 7 how to interpolate between the double regular n-gon and the right angled staircase. This step relies on the fact that the fundamental domain for the Veech group of the double regular n-gon has a simple shape, so that we can make explicit computations.

1.5. Organization of the paper

In Section 2 we recall prerequisites on translation surfaces, Veech groups, Veech surfaces, and we describe the right-angled staircase models for our surfaces. In Section 3 we explain why KVol is bounded on some Teichmüller curves. In Section 4 and Section 5 we explain how to interpret KVol geometrically, in terms of hyperbolic distance on the Teichmüller curve (identified with a quotient of $\mathbb{H}^2$ by a Fuchsian group), and we give an upper bound for KVol on the Teichmüller curve. In particular this proves that the maximum is achieved by the staircase surfaces.

Note that the results of Section 4 as well as Proposition 5.1 are not specific to the Teichmüller curve of the double regular $n-$gon.

In Section 6 we perform the first main step of the proof: we compute KVol for the double n-gon, by a geometric method, carefully looking at how saddle connections intersect depending on their directions.

In Section 7 we perform the second main step of the proof: we interpolate, by analytical methods, between the double n-gon and the staircase surfaces, thus proving that the minimum is achieved, uniquely, by the former.

Acknowledgments

The authors would like to thank the referee for several useful suggestions.

2. Double $n-$gons and staircase models

This section collects background material on the flat geometry of the double $n-$gons. We assume that the reader is familiar with basic notions about flat geometry, such as the $\mathrm{GL}(2,\mathbb{R})$-action and Veech groups and Teichmüller curves. General references for this include the surveys [Mas22, Wri16, Zor06].

2.1. Preliminaries

Let X be a translation surface. We denote the holonomy vector of a saddle connection α on X by $\overrightarrow{\alpha} = \int_\alpha \omega \in \mathbb{R}^2$. By abuse of notation we will often confuse $\overrightarrow{\alpha}$ with α. We have $l(\alpha) = \|\overrightarrow{\alpha}\|$. A horizontal cylinder $\mathcal{C}(w,h)$ is an euclidean annulus of the form $[0,w]\times(0,h)/(0,x)\sim(w,x)$. The parameters w and h are called, respectively, circumference and height of the cylinder. An open subset $\mathcal{C}\subset X$ is called a cylinder in direction θ if $e^{i\theta}\mathcal{C}$ is isomorphic to $\mathcal{C}(w,h)$ for some parameters w,h. We will say that w and h are the circumference and height of $\mathcal{C}$. The modulus of the cylinder is the ratio h/w.

The action of $\mathrm{SL}(2,\mathbb{R})$ on moduli spaces provides a powerful tool to study the dynamics of the translation flow on X. On the level of surfaces, any $A\in\mathrm{SL}(2,\mathbb{R})$ induces an affine homeomorphism $f: X\to A\cdot X$ such that the derivative map Df of f equals A.

Remark 2.1. — Since f is affine, it maps saddle connections of X to saddle connections of $A\cdot X$. Observe also that orientation-preserving homeomorphisms of surfaces preserve the intersection form.

We denote by $\mathrm{Aff}(X)$ (respectively $\mathrm{Aff}^+(X)$) the group of affine (respectively, orientation preserving) homeomorphisms of X, that is the group of affine homeomorphisms from X to itself. The derivative map provides a homomorphism from $\mathrm{Aff}^+(X)$ to $\mathrm{GL}^+(2,\mathbb{R})$. Its range coincides with the Veech group $\mathrm{SL}(X)$ of X.

2.2. The staircase model for the double $n-$gon

In this section, we review the flat geometry of the Veech examples [Vee89], and their different models. The constructions below are contained in [Hoo13, Mon05] and [FL23, Section 6.6.1]).

Originally, for $n\geqslant 3$, the Veech examples come from the unfolding construction of the right-angled triangles with angles $(\pi/2,\pi/n,(n-2)\cdot\pi/2n)$. We denote the associated surface by X_0.

- If $n\geqslant 8$ is even then X_0 is the quotient of the regular $n-$gon (with radius 1) by gluing obvious opposite sides by translation. The genus of X_0 is $\lfloor n/4\rfloor$. Moreover, if $n\equiv 0 \mod 4$ then X_0 has a unique singularity, otherwise it has two singularities of the same degree.
- If $n\geqslant 5$ is odd, then X_0 is the quotient of the double of the regular $n-$gon (with radius 1) by gluing obvious opposite sides by translation. It has a unique singularity and genus $(n-1)/2$.

As mentioned in the introduction we will focus on the latter case and in the sequel we will assume $n = 2m + 1$ is an odd integer.

The double n-gon X_0 has a staircase model S_0 in its $\mathrm{GL}(2, \mathbb{R})$-orbit, drawn in Figure 2.1 and described in [Hoo13] or [Mon05] (see also [Vee89, §5] or [Bou22]).

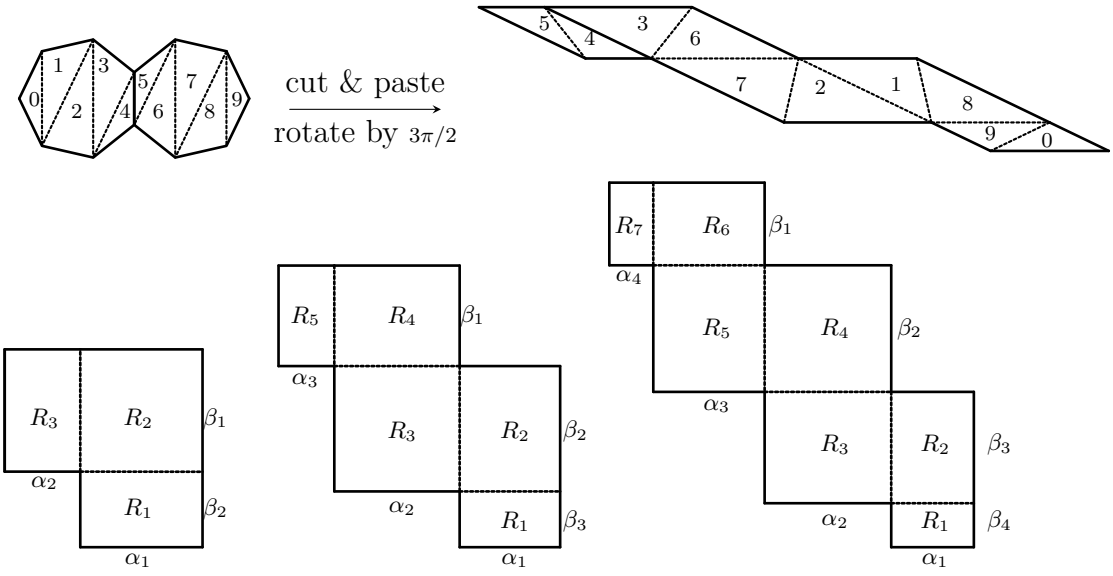

Figure 2.1. Above, the double $(2m+1)-$gon X_0 is cut into $2(2m-1)$ triangles, which are re-arranged into a slanted stair-shape, whose slanted sides are then rotated and sheared to create the right-angled stair-shape S_0. Below, a staircase model S_0 for X_0 ($n = 2m+1$), for $m = 2, 3, 4$, with saddle connections $(\alpha_i, \beta_i)_{i=1,\dots,m}$. The surface S_0 for $m = 2$ is usually shown rotated by 180 degrees, as the golden L (see [DFT11, DL18]*).*

Specifically, the staircase surface S_0 is made from a chain of $n-2$ rectangles $R_1, \dots, R_{n-2}$ where the sides of R_k are identified to the sides of R_{k+1} and R_{k-1}. The horizontal sides of R_{n-2} (resp. the vertical sides of R_1) are identified together. In particular, for $k = 2, \dots, n-2$, the union of the rectangles R_{k-1} and R_k is a horizontal cylinder whose core curve is homologous to the union of the saddle connections α_k and α_{k-1}. Its vertical boundary is β_{m-k+1}. With the notations of Figure 2.1, the lengths of saddle connections satisfy the equations

$$l(\alpha_k) = l(\beta_k) = \sin \frac{2k\pi}{n}, \text{ for any } k = 1, \dots, m, \tag{2.1}$$

and in particular one easily computes:

$$\mathrm{Vol}(S_0) = \frac{n}{2} \cos \frac{\pi}{n}. \tag{2.2}$$

The surface S_0 is decomposed into m horizontal cylinders. In order to exhibit the Veech group and a fundamental domain, one needs to compute the moduli of the m horizontal cylinders of S_0.

For $k = 1, \dots, m$, the core curve of the kth cylinder of S_0 is given by $\alpha_{k-1} + \alpha_k$ (with the dummy condition $\alpha_0 := 0$), and its height is β_{m-k+1}. It is easily seen that all moduli are the same and equal to

$$\frac{\text{height}}{\text{width}} = \frac{\sin\frac{2(m-k+1)\pi}{n}}{\sin\frac{2(k-1)\pi}{n} + \sin\frac{2k\pi}{n}} = \frac{\sin\frac{(2k-1)\pi}{n}}{2\sin\frac{2(k-1+k)\pi}{2n}\cos\frac{2(k-1-k)\pi}{2n}} = \frac{1}{2\cos\pi/n}.$$

From this knowledge, we can apply the Thurston–Veech construction, and obtain an affine homeomorphism of S_0 whose derivative map (outside the singularity) is a parabolic element of $\mathrm{SL}_2(\mathbb{R})$. More precisely the affine homeomorphism acts as a Dehn twist in each horizontal cylinder R_k for $k = 1, \dots, n-2$.

2.3. Veech group and fundamental domain

In this section, we describe the Veech group of S_0. For $n \geqslant 3$, we denote by Γ_n the Hecke triangle group of level n (or signature $(2, n, \infty)$) generated by

$$T = \begin{pmatrix} 1 & \Phi_n \\ 0 & 1 \end{pmatrix} \text{ and } R = \begin{pmatrix} 0 & -1 \\ 1 & 0 \end{pmatrix}, \text{ setting } \Phi_n = 2\cos\frac{\pi}{n}.$$

In the following we will simply use the notation Φ for Φ_n. It follows from [Vee89] that the Veech group of S_0 coincides with Γ_n.

The group Γ_n, acting on the hyperbolic plane $\mathbb{H}^2$, has a fundamental domain $\mathcal{D}$ depicted in Figure 2.2. It is comprised between the vertical geodesics with abscissae $-\Phi/2$ and $\Phi/2$, and the geodesic with endpoints ± 1. In the fundamental domain the staircase model S_0 is represented by the point i, while X_0 corresponds to the lower corners of $\mathcal{D}$ (the intersection between a vertical boundary and the circular boundary).

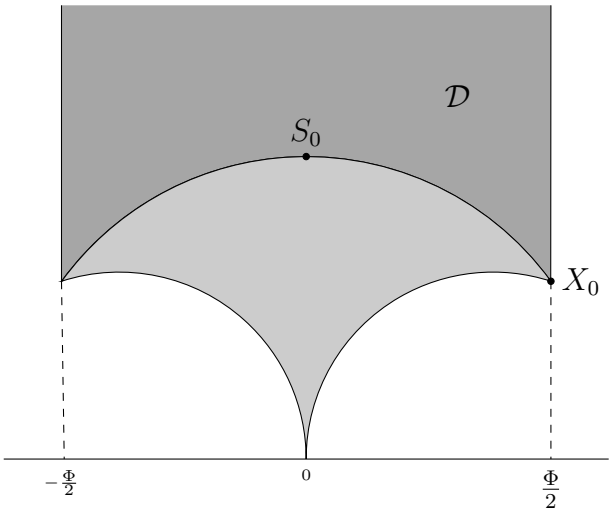

Figure 2.2. A fundamental domain $\mathcal{D}$ of the Veech group of the staircase model of the double regular $(2m+1)$-gon, along with its reflection in the geodesic $(-1, 1)$.

3. Boundedness of KVol on Teichmüller discs

In this section we consider translation surfaces with only one singularity.

Before studying the maximum of KVol on Teichmüller discs, we prove Theorem 1.7 which gives a criterion to ensure that it is indeed a bounded function. We conclude this section with a proof of Theorem 1.8.

To begin with, observe that if there are two parallel saddle connections α, β on X having non trivial intersection, then applying the Teichmüller geodesic flow in the orthogonal direction of α, β, we get for all $t > 0$

$$\mathrm{KVol}(g_t X) \geqslant \frac{1}{e^{-2t}|\alpha||\beta|}.$$

Thus KVol is not bounded on the Teichmüller disc of X. Actually, this remark applies to a large class of translation surfaces (of genus at least two): those decomposed into a single metric cylinder, as we will see below.

Before proving Theorem 1.7, we recall the notion of the angle of a horizontal saddle connection on a surface whose horizontal foliation has only closed leaves. The union of all (horizontal) saddle connections and the singularity defines a finite oriented graph. Orientation on the edges comes from the canonical orientation of the horizontal foliation. At the singularity p the directions of saddle connections attached to p alternate between incoming and outgoing as we follow the clockwise order. For a saddle connection γ one can count the number of different sectors between the two directions it determines. This gives an angle $(2k+1)\pi$ well defined modulo $2(2m-1)\pi$. Observe that if γ has angle π then it is the boundary of a metric cylinder embedded into the surface.

Lemma 3.1. — *Let X be a translation surface with only one singularity. If X has a cylinder decomposition all of whose boundary saddle connections have pairwise trivial intersection, then there is a saddle connection with angle π. In particular if X has a one cylinder decomposition and* $\mathrm{genus}(X) > 1$ *then there are two parallel saddle connections intersecting non trivially.*

For a more general statement, see [Bou23b, Théorème D, Theorem 5.1.5].

Proof of Lemma 3.1. — We consider a saddle connection γ having the smallest angle $(2k+1)\pi$ at p (see Figure 3.1). Assume $k > 0$. Then γ determines $2k+1$ sectors and so $2k$ saddle connections $\beta_1, \ldots, \beta_{2k}$. Since the angle of γ is minimal, no β_i can begin and end inside the sector of angle $(2k+1)\pi$ cut by γ. Therefore the intersection of β_i with γ is non trivial for every $i = 1, \ldots, k$.

□

From this observation and the fact that one-cylinder surfaces are dense, we immediately deduce that KVol is not bounded on any connected component of the moduli space of translation surfaces of genus $m \geqslant 2$, with a single singularity. Similarly, since KVol is a continuous function, it is not bounded on the Teichmüller disc of a generic (with respect to the Masur–Veech measure) surface X. Veech surfaces are exceptionally symmetric translation surfaces and are not generic if $m \geqslant 2$. Theorem 1.7 deals with those surfaces.

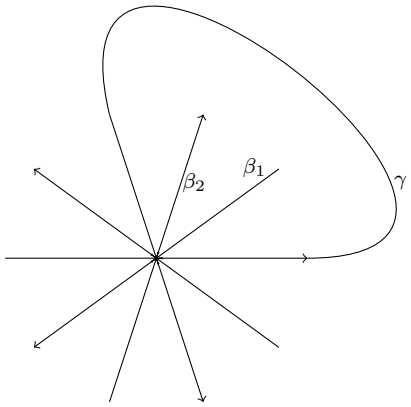

Figure 3.1. A separatrix diagram of a genus 4 surface. The singularity p has conical angle 10π and γ has angle 3π (or 7π modulo 10π).

Proof of Theorem 1.7. — As already mentioned at the beginning of this section, KVol is not bounded if there are parallel saddle connections intersecting non-trivially, and hence we only need to prove the "if" part of the theorem.

Let us consider only surfaces which have total area 1. Let X be a Veech surface with a unique singularity. We recall that for such X the supremum in the definition of KVol can be taken over saddle connections, see Remark 1.3.

Let θ be the angle associated to two periodic directions (d, d') having saddle connections α, β with nontrivial intersections. The hypothesis that parallel saddle connections do not intersect ensures that $d \neq d'$, so that up to swapping d and d' we may assume $\theta \in]0, \pi[$. Then, any intersection between a saddle connection α with direction d, and a saddle connection β with direction d', if it occurs outside the singularity, is positive. Therefore, given two saddle connections α and β, with respective directions d and d', either $\mathrm{Int}(\alpha, \beta) = -1$, in which case α and β intersect only once, at the singularity, or $\mathrm{Int}(\alpha, \beta) \geqslant 0$.

Let $\alpha_1, \ldots, \alpha_r$ be the saddle connections in direction d. By Veech dichotomy, X is decomposed into cylinders $C_1, \ldots, C_s$ (of heights $h_1(d), \ldots, h_s(d)$) with direction d. Observe that since X has genus m and a unique singularity, the number s of cylinders is bounded by the genus m of the surface. We can subdivide β each time it intersects the α_k, and count the length of each segment we obtain. This gives:

$$l(\beta) \cdot \sin\theta = \sum_{k=1}^{r} h_k(d)\mathrm{Int}(\alpha_k, \beta) = \sum_{k=1}^{r} c_k(d)\frac{\mathrm{Int}(\alpha_k, \beta)}{l(\alpha_k)}, \tag{3.1}$$

where $c_k(d) = h_k(d) \cdot l(\alpha_k)$ represents the area of an embedded parallelogram supported on α_k. We write $l(\alpha_k)l(\beta) = \alpha_k \wedge \beta / \sin\theta$, so

$$1 = \sum_{k=1}^{r} c_k(d)\frac{\mathrm{Int}(\alpha_k, \beta)}{\alpha_k \wedge \beta}.$$

Writing in a slightly different way:

$$1 = \sum_{\substack{k \\ \mathrm{Int}(\alpha_k,\beta) \geqslant 0}} c_k(d) \frac{\mathrm{Int}(\alpha_k,\beta)}{\alpha_k \wedge \beta} - \sum_{\substack{k \\ \mathrm{Int}(\alpha_k,\beta)=-1}} \frac{c_k(d)}{\alpha_k \wedge \beta}.$$

By [Vor96], there are no small triangles in X i.e. there exists $M > 0$, depending only on X, such that $|\alpha_k \wedge \beta| > M$ (this is actually the easy part of the characterization of Veech surfaces in [SW10]). In particular since $c_k(d) \leqslant \mathrm{Area}(X) = 1$, we have

$$\sum_{\substack{k \\ \mathrm{Int}(\alpha_k,\beta)=-1}} \frac{c_k(d)}{\alpha_k \wedge \beta} < r \cdot \frac{1}{M} < C$$

for some uniform constant $C = C(X)$ (recalling $r \leqslant m$). Thus

$$\frac{\mathrm{Int}(\alpha_k,\beta)}{\alpha_k \wedge \beta} < \frac{1+C}{c_k(d)} < \frac{1+C}{M}.$$

Hence $\dfrac{\mathrm{Int}(\alpha_k,\beta)}{l(\alpha_k)l(\beta)}$ is uniformly bounded on the Teichmüller disc of X. Since $\mathrm{Area}(X) = 1$, KVol is uniformly bounded as well. □

In genus 2 we have a more precise description.

Proof of Theorem 1.8. — By [McM07], in the stratum $\mathcal{H}(2)$, Teichmüller discs are either dense or closed. So if X is not a Veech surface, KVol is not bounded from above on its Teichmüller disc. For Veech surfaces, a quick inspection of possible cylinder diagrams leads to the following observation: for two-cylinder decompositions, there are no parallel saddle connections with non trivial intersections. Now a Veech surface in genus two is either primitive or square-tiled. By [McM05, Corollary A.2], square-tiled surfaces all admit one-cylinder decompositions. Since genus two primitive Veech surfaces do not have one-cylinder decompositions, we get the desired result. □

4. $\mathrm{SL}(2,\mathbb{R})-$action and directions in the Teichmüller disc

In this section we analyze the action of affine homeomorphisms on the set of saddle connections.

If X is a translation surface, and $A \in \mathrm{GL}^+(2,\mathbb{R})$ we denote by $f : X \to A \cdot X$ the corresponding affine map. By Remark 2.1 f preserves the intersection form. Saddle connections of X are mapped to saddle connections of $A \cdot X$, but lengths are not preserved in general. The right quantity to consider is not the length of α or β but rather the quantity $\overrightarrow{\alpha} \wedge \overrightarrow{\beta} = l(\alpha)l(\beta)\sin\theta$, where θ is the angle between the holonomy vectors $\overrightarrow{\alpha}$, $\overrightarrow{\beta}$ associated to α, β. The wedge product is invariant under $\mathrm{SL}(2,\mathbb{R})$ and is twice the area of a (virtual) triangle delimited by α and β.

Remark 4.1. — In general we cannot identify f with its derivative map $Df \in \mathrm{GL}^+(2,\mathbb{R})$. The reason is that there might be affine maps whose derivative map is trivial. Equivalently the group $\mathrm{Aff}(X)$ is only virtually isomorphic to the Veech group $\mathrm{SL}(X)$, up to the group of automorphism $\mathrm{Aut}(X)$. In our situation, since there

is only one singularity, $\mathrm{Aut}(X)$ is trivial, and we will implicitly identify matrices with affine homeomorphisms.

The above observation motivates the following definition.

Definition 4.2. —

- *For $d \in \mathbb{R}P^1$, we say that a saddle connection in S_0 has direction d if it has direction d in the plane template of Figure 2.1.*
- *For $M \in \mathrm{GL}^+(2,\mathbb{R})$ we say that a saddle connection α in $M \cdot S_0$ has direction d if $M^{-1} \cdot \alpha$ has direction d in S_0*

Roughly speaking, we prefer to see each saddle connection α on $M \cdot S_0$ as coming from a saddle connection $M^{-1}\alpha$ on S_0, and we define the direction of α accordingly. For this reason we refer to S_0 as the *base surface* of the orbit. Although this choice is arbitrary, choosing the staircase model S_0 as base surface will turn out to be convenient. This way of labelling directions is a bit counter-intuitive because α may not have direction d in a plane template for $M \cdot S_0$, but it makes sense with the following statement.

Proposition 4.3. — *Using the identifications*[(1)]

$$\Psi : d = [x : y] \in \mathbb{R}P^1 \mapsto -\frac{x}{y} \in \mathbb{R} \cup \{\infty\} \simeq \partial\mathbb{H}^2$$

and, for $M = \left(\begin{smallmatrix} m_{1,1} & m_{1,2} \\ m_{2,1} & m_{2,2} \end{smallmatrix}\right) \in \mathrm{SO}(2,\mathbb{R})\backslash\mathrm{GL}^+(2,\mathbb{R})$,

$$\chi : M \cdot S_0 \in \mathcal{T}_n \mapsto \frac{m_{2,2}i + m_{1,2}}{m_{2,1}i + m_{1,1}} \in \mathbb{H}^2,$$

the locus of surfaces in $\mathcal{T}_n$ where the directions d and d' make an (unoriented) angle $\theta \in]0, \frac{\pi}{2}]$ is the banana neighbourhood

$$\gamma_{d,d',r} = \left\{ z \in \mathbb{H}^2 : d_{\mathrm{hyp}}(z, \gamma_{d,d'}) = r \right\}$$

where $\cosh r = \frac{1}{\sin\theta}$, $\gamma_{d,d'}$ denotes the hyperbolic geodesic with endpoints $\Psi(d)$ and $\Psi(d')$, and d_{hyp} is the hyperbolic distance.

In particular, the locus of surfaces in $\mathcal{T}_n$ where the directions d and d' are orthogonal is the hyperbolic geodesic with endpoints $\Psi(d)$ and $\Psi(d')$.

To simplify notations we will omit the reference to Ψ, and d will either denote d or $\Psi(d)$ depending on the context. Similarly we will denote by $\gamma_{d,d'}$ the hyperbolic geodesic with endpoints $\Psi(d)$ and $\Psi(d')$.

Notation 4.4. — In the rest of the paper, we denote by $\theta(X, d, d')$ the angle between the directions d and d' in the surface $X = M \cdot S_0$. Notice that Proposition 4.3 gives

$$\cosh d_{hyp}(X, \gamma_{d,d'}) = \frac{1}{\sin\theta(X, d, d')}.$$

(1) Note that χ defines a right action of $\mathrm{GL}^+(2,\mathbb{R})$. See [Mas22, Section 6.1], as to why we should quotient by $\mathrm{SO}(2,\mathbb{R})$ on the left, and act by $\mathrm{GL}^+(2,\mathbb{R})$ on the right.

Proof of Proposition 4.3. — For $\theta \in]0, \frac{\pi}{2}]$ and $u, v \in \mathbb{R}^2$ with equivalence classes $d \neq d'$ we define

$$\mathcal{M}(d, d', \theta) = \left\{ M \in GL^+(2, \mathbb{R}) : \min\Big(\text{angle}(\pm Mu, \pm Mv), \text{angle}(\pm Mv, \pm Mu)\Big) = \theta \right\}.$$

Observe that $\mathcal{M}(d, d', \theta)$ is well defined (it only depends on the equivalence classes d, d' because the angles are taken modulo π) and equivariant by right multiplication: if $G \in GL^+(2, \mathbb{R})$ then

$$\mathcal{M}(d, d', \theta).G = \mathcal{M}\left(G^{-1}d, G^{-1}d', \theta\right). \tag{4.1}$$

Denote $\bar{\mathcal{M}}(d, d', \theta)$ the projection of $\mathcal{M}(d, d', \theta)$ to $\mathbb{H}^2$. Observe that $\mathcal{M}(d, d', \theta)$ is invariant by left multiplication by $SO(2, \mathbb{R})$, so any matrix in $GL^+(2, \mathbb{R})$ that projects to an element of $\bar{\mathcal{M}}(d, d', \theta)$, is actually in $\mathcal{M}(d, d', \theta)$.

Let us look at the case $d = (\bar{1}) = \infty$ and $d' = (\bar{0}) = 0$. Observe that in that case $\bar{\mathcal{M}}(d, d', \theta)$ is invariant by $z \mapsto \lambda z$, for any $\lambda > 0$. Indeed, take $\lambda > 0$ and $z \in \bar{\mathcal{M}}(d, d', \theta)$, and let M

be an element of $\mathcal{M}(d, d', \theta) \subset GL^+(2, \mathbb{R})$ which projects to z. Then the matrix

$$M' = M \cdot \begin{pmatrix} 1 & 0 \\ 0 & \lambda \end{pmatrix} \in GL^+(2, \mathbb{R})$$

projects to λz. But the equivalence class, in $\mathbb{R}P^1$, of $\left(\begin{smallmatrix} 1 & 0 \\ 0 & \lambda \end{smallmatrix}\right)\left(\begin{smallmatrix} 1 \\ 0 \end{smallmatrix}\right)$ (resp. $\left(\begin{smallmatrix} 1 & 0 \\ 0 & \lambda \end{smallmatrix}\right)\left(\begin{smallmatrix} 0 \\ 1 \end{smallmatrix}\right)$), is d (resp. d'), and we have seen that $\mathcal{M}(d, d', \theta)$ only depends on the equivalence classes d, d', so $M \in \mathcal{M}(d, d', \theta)$ entails $M' \in \mathcal{M}(d, d', \theta)$. Therefore $\lambda z \in \bar{\mathcal{M}}(d, d', \theta)$.

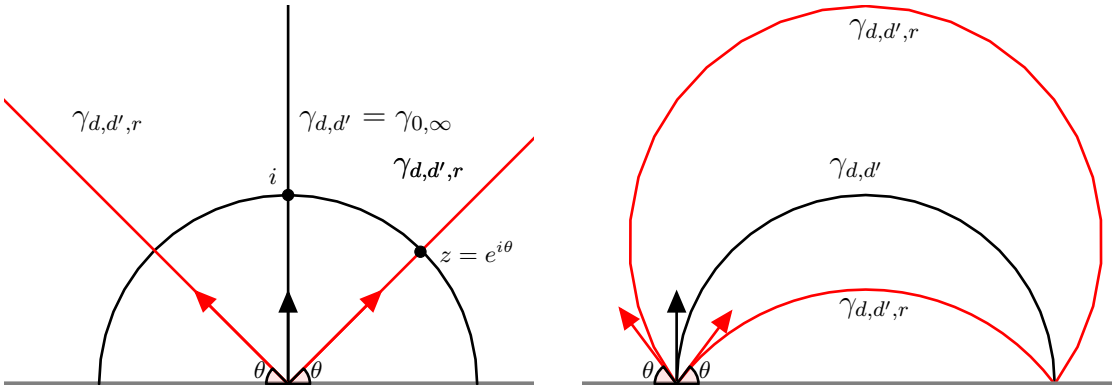

Figure 4.1. The set $\gamma_{d,d',r}$ for $\cosh r = \frac{1}{\sin\theta}$.

Thus, to determine $\bar{\mathcal{M}}(d, d', \theta)$, it suffices to determine its intersection with the horizontal straight line $\{y = 1\}$, which we parametrize as

$$\left\{ i + \cot\alpha : \alpha \in]0, \pi[\right\}$$

A corresponding set of matrices in $GL^+(2, \mathbb{R})$ is given by

$$\left\{ \begin{pmatrix} 1 & \cot\alpha \\ 0 & 1 \end{pmatrix} : \alpha \in]0, \pi[\right\}$$

which sends $\binom{1}{0}$ and $\binom{0}{1}$ to, respectively, $\binom{1}{0}$ and $\binom{\cot\alpha}{1}$. The angle of the latter vectors is α, so $\bar{\mathcal{M}}(d,d',\theta)\cap\{y=1\}=\{\binom{\cot\theta}{1}\}$. Therefore, $\bar{\mathcal{M}}(d,d',\theta)$ is the half-line which starts at the origin, with co-slope $\cot\theta$. This is precisely $\gamma_{d,d',r}$ with $\cosh r=\frac{1}{\sin\theta}$, since the hyperbolic distance from $z=e^{i\theta}$ to the geodesic $\gamma_{0,\infty}$ is realized by the geodesic η parameterized by $\eta(t)=e^{it}$ for $t\in[\theta,\pi/2]$, so that by definition

$$r=\mathrm{d}_{hyp}(z,\gamma_{d,d'})=l_{\mathrm{hyp}}(\eta)=\int_\theta^{\pi/2}\frac{dt}{\sin t}=\frac{1}{2}\log\frac{1+\cos\theta}{1-\cos\theta},$$

thus $\cos\theta=\frac{e^{2r}-1}{e^{2r}+1}$, and

$$\sin\theta=\sqrt{1-\cos^2\theta}=\sqrt{1-\left(\frac{e^{2r}-1}{e^{2r}+1}\right)^2}=\frac{2e^r}{e^{2r}+1}=\frac{1}{\cosh r}.$$

Now let us consider the general case. Pick $G\in GL^+(2,\mathbb{R})$ taking directions d,d' to $\binom{\bar{1}}{0}=\infty$ and $\binom{\bar{0}}{1}=0$ respectively. Then, by Equation (4.1), $\mathcal{M}(\infty,0,\theta).G=\mathcal{M}(d,d',\theta)$, so $\bar{\mathcal{M}}(d,d',\theta)$ is the image of $\bar{\mathcal{M}}(\infty,0,\theta)$ by the orientation-preserving isometry of $\mathbb{H}^2$ corresponding to the action of G. One verifies that this isometry sends ∞ and 0 to the images of the directions d and d' by the identification $\mathbb{R}P^1\simeq\partial\mathbb{H}^2$ via the opposite of the co-slope, respectively. This finishes the proof of Proposition 4.3. □

5. Another look at KVol

Recall that the function KVol can be expressed as a supremum over saddle connections α,β in (1.1). We will use the invariance of $\mathrm{Int}(\cdot,\cdot)$ for the action of affine homeomorphisms on translation surfaces and the invariance of $\wedge$ for the linear action of $\mathrm{SL}(2,\mathbb{R})$ on $\mathbb{R}^2$ in order to have a more suitable formula to work with. In the sequel we will use the notation $K(X)$:

$$\mathrm{KVol}(X)=\mathrm{Vol}(X)\cdot K(X).$$

Proposition 5.1. — *Let $\mathcal{P}$ be the set of periodic directions in $X=M\cdot S_0$ for some $M\in\mathrm{SL}(2,\mathbb{R})$. Then*

$$K(X)=\sup_{\substack{d,d'\in\mathcal{P}\\ d\neq d'}}K(d,d')\cdot\sin\theta(X,d,d'),$$

where $K(d,d')=\sup\{\frac{\mathrm{Int}(\alpha,\beta)}{\alpha\wedge\beta}\mid\begin{smallmatrix}\alpha\subset S_0\ \text{in direction } d\\ \beta\subset S_0\ \text{in direction } d'\end{smallmatrix}\}$ and $\theta(X,d,d')$ is the angle given in Notation 4.4.

Remark 5.2. — Although Definition 4.2, Proposition 4.3 and Proposition 5.1 are stated here for the Teichmüller disk of the double regular n-gon with base surface S_0, they can be generalized to any Teichmüller disk of surfaces with a unique singularity. Proposition 4.3 does not require any additional assumption whereas we need to assume that parallel saddle connections are pairwise non intersecting in order to generalize Proposition 5.1. Notice that this condition (which is the boundedness

condition of Theorem 1.7) does not depend of the choice of base surface in the Teichmüller disk.

Observe that the quantity $K(d,d')$ is invariant under the diagonal action of the Veech group Γ. Moreover $\sin\theta(X,d,d') = 1/\cosh r$, where r is the hyperbolic distance between X and the geodesic $\gamma_{d,d'}$, by Proposition 4.3.

Proof of Proposition 5.1. — Given two saddle connections $\alpha, \beta \subset X$ having directions d, d' (in X) and making an angle θ, one has $\alpha \wedge \beta = l(\alpha)l(\beta)\sin\theta$. Notice that parallel saddle connections do not intersect in X, so we will assume $d \neq d'$. By definition these saddle connections are the images by M of saddle connections $\alpha', \beta' \subset S_0$ having directions d, d' (in S_0), and thus $M \in \mathcal{M}(d,d',\theta)$. In particular the projection of M to $\mathbb{H}^2$, that is $X \in \bar{\mathcal{M}}(d,d',\theta)$, gives $\theta = \theta(X,d,d')$. Now, by definition (see (1.1)),

$$\begin{aligned}
&\sup_{\alpha,\beta} \frac{\mathrm{Int}(\alpha,\beta)}{l(\alpha)l(\beta)} \\
&\qquad = \sup_{\substack{d,d'\in\mathcal{P}\\ d\neq d'}} \sup_{\substack{\alpha\subset X \text{ in direction } d\\ \beta\subset X \text{ in direction } d'}} \frac{\mathrm{Int}(\alpha,\beta)}{l(\alpha)l(\beta)} \\
&\qquad = \sup_{\substack{d,d'\in\mathcal{P}\\ d\neq d'}} \sup_{\substack{\alpha\subset X \text{ in direction } d\\ \beta\subset X \text{ in direction } d'}} \frac{\mathrm{Int}(\alpha,\beta)}{\alpha\wedge\beta}\cdot \sin \mathrm{angle}(\alpha,\beta) \\
&\qquad = \sup_{\substack{d,d'\in\mathcal{P}\\ d\neq d'}} \sup_{\substack{M^{-1}\alpha\subset S_0 \text{ in direction } d\\ M^{-1}\beta\subset S_0 \text{ in direction } d'}} \frac{\mathrm{Int}(M^{-1}\alpha,M^{-1}\beta)}{M^{-1}\alpha\wedge M^{-1}\beta}\cdot \sin\theta(X,d,d') \\
&\qquad = \sup_{\substack{d,d'\in\mathcal{P}\\ d\neq d'}} K(d,d')\cdot\sin\theta(X,d,d')
\end{aligned}$$

as desired. □

We end this section with the computation of $K(0,\infty)$ and $K(0,\Phi)$, for later use.

Proposition 5.3. — *The following hold:*

(i) $K(0,\infty) = \frac{1}{l(\alpha_m)^2}$ *and* $K(0,\Phi) = \frac{1}{\Phi}\cdot K(0,\infty)$.
(ii) $\forall\ (d,d') \notin \Gamma_n\cdot(0,\infty)$, $K(d,d') \leqslant K(0,\Phi)$.

Remark 5.4. — A direct consequence of Proposition 5.3 (combined with Proposition 5.1) is that for every $X \in \mathcal{T}_n$ such that $\sin\theta(X,0,\infty) \geqslant \frac{1}{\Phi}$, we have

$$K(X) = K(0,\infty)\cdot\sin\theta(X,0,\infty).$$

This is for example the case for every right angled staircase, which are represented via χ as elements of the hyperbolic geodesic $\gamma_{0,\infty}$, and for which we have $\sin(X,0,\infty) = 1$.

Proof of Proposition 5.3. —
(i) We use the notations of Figure 2.1. The directions $d = 0$ and $d' = \infty$ correspond to the vertical and the horizontal, respectively. By definition

$$K(0,\infty) = \sup_{\substack{\alpha \subset S_0 \text{ vertical} \\ \beta \subset S_0 \text{ horizontal}}} \frac{\mathrm{Int}(\alpha,\beta)}{l(\alpha)l(\beta)} = \sup_{i,j=1,\dots,m} \frac{\mathrm{Int}(\alpha_i,\beta_j)}{l(\alpha_i)l(\beta_j)}$$

Since the α_i and the β_j are saddle connections that can only intersect at the singularity, we have $\mathrm{Int}(\alpha_i,\beta_j) \in \{0,\pm 1\}$. Moreover, $l(\alpha_k) = l(\beta_k) = \sin 2k\pi/(2m+1) \geqslant \sin \pi/(2m+1)$ and equality is realized for $k = m$. From $\mathrm{Int}(\alpha_m,\beta_m) \neq 0$, we draw

$$K(0,\infty) = \frac{1}{l(\alpha_m)l(\beta_m)} = \frac{1}{l(\alpha_m)^2}.$$

The discussion for the directions $d = 0$ and $d' = \Phi$ is similar. They correspond to the vertical and the direction of the diagonal of horizontal cylinders. It is clear that

$$K(0,\Phi) = \sup_{\substack{\alpha \subset S_0 \text{ vertical} \\ \beta \subset S_0 \text{ diagonal of a horizontal cylinder}}} \frac{\mathrm{Int}(\alpha,\beta)}{l(\alpha)l(\beta)}$$

is maximal for $\alpha = \beta_m$ and $\beta = \alpha_1 + \beta_m$. And we have $K(0,\Phi) = \frac{\mathrm{Int}(\alpha,\beta)}{\alpha\wedge\beta} = \frac{1}{l(\alpha_1)l(\beta_m)} = \frac{1}{\Phi}K(0,\infty)$.
(ii) Let $(d,d') \notin \Gamma\cdot(0,\infty)$. Since $K(d,d')$ is invariant under the diagonal action of the Veech group and d is a periodic direction, we can assume $d = \infty$, and, up to a horizontal shear, $d' \in]0,\Phi[$. Notice that given a geodesic β in direction d', every intersection with any of the α_i requires a vertical length $l(\alpha_1)$ (this is where we use the fact that d' is not vertical), that is

$$\forall\, i \in \{1,\cdots,m\},\ l(\beta)\sin\theta(S_0,d,d') \geqslant l(\alpha_1)\mathrm{Int}(\alpha_i,\beta).$$

Hence

$$\forall\, i \in \{1,\cdots,m\},\ \frac{\mathrm{Int}(\alpha_i,\beta)}{l(\alpha_i)l(\beta)\sin\theta(S_0,d,d')} \leqslant \frac{1}{l(\alpha_1)l(\alpha_i)}$$

But $l(\alpha_i)l(\beta)\sin\theta(S_0,d,d') = \alpha_i \wedge \beta$, and $l(\alpha_i) \geqslant l(\alpha_m)$, so that the last equation reduces to

$$\forall\, i \in \{1,\cdots,m\},\ \frac{\mathrm{Int}(\alpha_i,\beta)}{\alpha_i\wedge\beta} \leqslant \frac{1}{l(\alpha_1)l(\alpha_m)} = \frac{1}{\Phi}K(0,\infty),$$

where the last equality follows from (i). This concludes the proof of Proposition 5.3. □

6. Computation of KVol for the double $(2m+1)$-gon

In this section we show that $\mathrm{KVol}(X_0)$ is realised by pairs of sides of the double $(2m+1)$-gon:

PROPOSITION 6.1. — *For every pair of saddle connections α and β on X_0, we have:*

$$\frac{Int(\alpha,\beta)}{l(\alpha)l(\beta)} \leqslant \frac{1}{l_0^2}$$

where l_0 is the length of the side of the $(2m+1)$-gon.
Moreover, equality is achieved if and only if α and β are two distinct sides of the regular $(2m+1)$-gon.

In particular, since the directions $d=0$ and $d'=\infty$ represent sides of the double $(2m+1)$-gon, we deduce the following:

COROLLARY 6.2. — *For $X=X_0$ the double $(2m+1)$-gon, we have:*

$$K(X_0) = K(0,\infty)\cdot \sin\theta(X_0,0,\infty)$$

The main idea of the proof of Proposition 6.1 is to subdivide both saddle connections α and β into segments of length at least l_0 such that each segment of α intersect each segment of β at most once. While, strictly speaking, we do not achieve that, we still get estimates good enough for our purpose, see Lemma 6.8.

6.1. Sectors and transition diagrams

Let α and β be two saddle connections on the double $(2m+1)$-gon. We partition the set of possible directions into $2m+1$ sectors of angle $\frac{\pi}{2m+1}$, as in Figure 6.1 for the double heptagon.

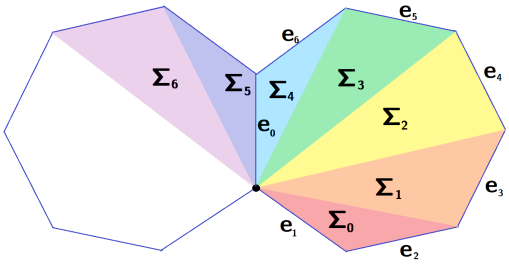

Figure 6.1. The seven sectors for the double heptagon.

To each sector Σ_i there is associated a *transition diagram* which encodes the admissible sequences of intersections with the sides of the double $(2m+1)$-gon, as in [DL18, §3] (See also [SU10, SU11] for the original description of sectors and transition diagrams, in the case of the regular octagon). Such a diagram looks like:

$$e_{\sigma_i(1)} \leftrightharpoons e_{\sigma_i(2)} \leftrightharpoons \cdots \leftrightharpoons e_{\sigma_i(2n)} \leftrightharpoons e_{\sigma_i(2m+1)}$$

with $\sigma_i \in \mathfrak{S}_{2m+1}$, and it means that for any curve α in sector Σ_i, each intersection of α with $e_{\sigma_i(j)}$ is preceded and followed by an intersection with either $e_{\sigma_i(j-1)}$ or $e_{\sigma_i(j+1)}$ [(2)]. In particular, each intersection with $e_{\sigma_i(1)}$ (resp. $e_{\sigma_i(2m+1)}$) is preceded

[(2)] Unless it reaches a singularity.

(and followed) by an intersection with $e_{\sigma_i(2)}$ (resp. $e_{\sigma_i(2m)}$). We say that the side $e_{\sigma_i(1)}$ (resp. $e_{\sigma_i(2m+1)}$) is *sandwiched* by $e_{\sigma_i(2)}$ (resp. $e_{\sigma_i(2m)}$) in the sector Σ_i.

For the sake of completeness, we provide the seven possible transition diagrams for the double heptagon.

$$\begin{aligned}
&\Sigma_0 : e_1 \leftrightharpoons e_2 \leftrightharpoons e_0 \leftrightharpoons e_3 \leftrightharpoons e_6 \leftrightharpoons e_4 \leftrightharpoons e_5\\
&\Sigma_1 : e_5 \leftrightharpoons e_6 \leftrightharpoons e_4 \leftrightharpoons e_0 \leftrightharpoons e_3 \leftrightharpoons e_1 \leftrightharpoons e_2\\
&\Sigma_2 : e_2 \leftrightharpoons e_3 \leftrightharpoons e_1 \leftrightharpoons e_4 \leftrightharpoons e_0 \leftrightharpoons e_5 \leftrightharpoons e_6\\
&\Sigma_3 : e_6 \leftrightharpoons e_0 \leftrightharpoons e_5 \leftrightharpoons e_1 \leftrightharpoons e_4 \leftrightharpoons e_2 \leftrightharpoons e_3\\
&\Sigma_4 : e_3 \leftrightharpoons e_4 \leftrightharpoons e_2 \leftrightharpoons e_5 \leftrightharpoons e_1 \leftrightharpoons e_6 \leftrightharpoons e_0\\
&\Sigma_5 : e_0 \leftrightharpoons e_1 \leftrightharpoons e_6 \leftrightharpoons e_2 \leftrightharpoons e_5 \leftrightharpoons e_3 \leftrightharpoons e_4\\
&\Sigma_6 : e_4 \leftrightharpoons e_5 \leftrightharpoons e_3 \leftrightharpoons e_6 \leftrightharpoons e_2 \leftrightharpoons e_0 \leftrightharpoons e_1
\end{aligned} \tag{6.1}$$

6.2. Construction of the subdivision

Let us denote by Σ_α (resp. Σ_β) the sector of α (resp. β), and σ_α (resp. σ_β) the corresponding permutation. Now, we cut α (resp. β) at each intersection with a non-sandwiched side in the sector Σ_α (resp. Σ_β). We get a decomposition $\alpha = \alpha_1 \cup \cdots \cup \alpha_k$ and $\beta = \beta_1 \cup \cdots \cup \beta_l$ with $k, l \geqslant 1$ and each segment is called sandwiched or non-sandwiched according to the following rules (see Figure 6.2):

- a segment which goes from one side to another non-adjacent side of one of the $(2m+1)$-gons is called non-sandwiched.
- a segment which intersects a sandwiched side in its interior is called sandwiched. Such segments go through both $(2m+1)$-gons (see Figure 6.3).
- an initial or final segment α_1, α_k, β_1, β_l is called non-sandwiched.

Notation 6.3. — When a segment α_i (or β_j) intersects the side e which is sandwiched by e' in the corresponding sector, we say that α_i is of type $e' \to e \to e'$.

Remark 6.4. — For a sandwiched segment α_i of type $e' \to e \to e'$, there is a parallelogram $P(e', e) \subset X_0$ with the following property: one of its sides is e' and one of its diagonals is e. The segment α_i goes from one e'-side to the opposite side. The closure of $P(e', e)$ is a cylinder.

Notice that for each sector Σ_i, the sides of the $(2m+1)$-gon which are sandwiched in Σ_i are those having direction in the boundary of Σ_i. For instance, the sides of the double heptagon which are sandwiched in the sector Σ_0 are e_1 and e_5 (see Figure 6.1).

Moreover, the side of the $(2m+1)$-gon with direction in $\Sigma_i \cap \Sigma_{i-1}$ is sandwiched in both sectors Σ_i and Σ_{i-1}, but in Σ_i it is sandwiched by its successor in the cyclic order (modulo $2m+1$), while in Σ_{i-1} it is sandwiched by its predecessor. For instance, e_1 is sandwiched by e_2 in Σ_0, while it is sandwiched by e_0 in Σ_{2m} (Σ_6 for the double heptagon).

Remark 6.5. — Since no two sectors have the same pair (sandwiched side, sandwiching side), prescribing the type of α_i automatically tells which sector the direction of α belongs to.

Remark 6.6. — If α is a diagonal of the double $(2m+1)$-gon, the sector is not uniquely defined. However, in such cases α is not divided into pieces and $k = 1$.

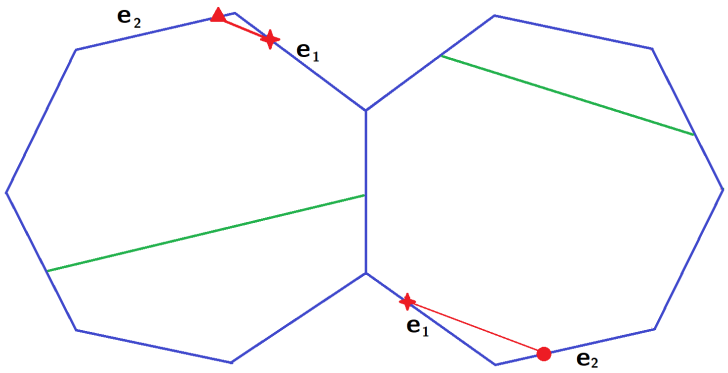

Figure 6.2. Examples of non-sandwiched segments in green and a sandwiched segment in red. The sandwiched segment is of type $e_2 \to e_1 \to e_2$. Remark that the points ◯ and △ on the side e_2 are not the same.

The next two lemmas are the reason for this peculiar way of subdividing saddle connections.

LEMMA 6.7. — *Every segment of α (resp. β) has length at least l_0, with equality if and only if α (resp. β) is a side of the double $(2m+1)$-gon.*

Proof. — A non-sandwiched segment goes from one side (or vertex) of a $(2m+1)$-gon to a *non-adjacent* side in the same $(2m+1)$-gon. So its length is at least l_0.

Now take a sandwiched segment α_i which intersects a sandwiched side e in its interior. If the type of α_i is $e' \to e \to e'$, then by Remark 6.4, α_i goes from the side e' of $P(e', e)$ to the opposite side of $P(e', e)$. In particular the length of α_i is no less than that of e' which is l_0. □

6.3. Study of the intersections

In this section, we investigate the possible intersections between the segments of α and β. First observe that α_i and β_j can have nontrivial intersections on the interior of the sides of a sector Σ_α. However if this happen, we can slightly deform α as follows. We change the slope of α_i and α_{i+1} so that the new segment α_i' intersects β_j in the interior of Σ_α the same number of times α_i intersects β_j. We choose the deformation small enough so that we do not create new intersections with the others segments. The new path $\alpha' = \alpha_1 \cup \cdots \cup \alpha_i' \cup \alpha_{i+1}' \cup \cdots \cup \alpha_k$ is homologous to α by construction. In the sequel we will simply write α instead of α'.

Now, since β is made of segments of straight lines in the same direction, and α is made of segments whose directions are close to a given direction, all non-singular intersections have the same sign. In particular, adding the possible singular intersection, it gives:

$$Int(\alpha, \beta) \leqslant \sum_{i,j} |Int(\alpha_i, \beta_j)| + 1 \tag{6.2}$$

where $|Int(\alpha_i, \beta_j)|$ is the geometric intersection between α_i and β_j.

LEMMA 6.8. — *If α and β are not both diagonals, then $Int(\alpha, \beta) \leqslant kl$.*

Proof of Lemma 6.8. — We will show that $\sum_{i,j} |Int(\alpha_i, \beta_j)| \leqslant kl - 1$. Let us fix i, j. We first observe that if either α_i or β_j is a non-sandwiched segment, then α_i and β_j intersect at most once (possibly on a side). Indeed a non-sandwiched segment goes from one side to another non-adjacent side of one of the $(2m + 1)$-gons. In particular it is a segment that is contained entirely in one of the $(2m + 1)$-gons. A sandwiched segment consists of two straight segments, not contained in the same $(2m + 1)$-gon. Hence in total they intersect at most once.

Thus it remains to consider the case where α_i and β_j are sandwiched segments. Up to a rotation and a symmetry, we can assume α_i is of type $e_2 \to e_1 \to e_2$ (see Figure 6.1). The sector determined by α is necessarily Σ_0.

Now if β_j is sandwiched but neither e_1 nor e_2 appear in the type of β_j, then β_j is contained in the parallelogram $P(e_k, e_l)$ (defined in Remark 6.4) for some $e_k, e_l \notin \{e_1, e_2\}$. In particular α_i does not intersect this parallelogram, and neither does it intersect β_j.

Eventually it remains to treat the following cases where β_j is of type:

$(1) e_0 \to e_1 \to e_0$ $(2) e_1 \to e_0 \to e_1$

$(3) e_1 \to e_2 \to e_1$ $(4) e_2 \to e_1 \to e_2$

$(5) e_2 \to e_3 \to e_2$ $(6) e_3 \to e_2 \to e_3$

In all situations but (3), we can show that α_i and β_j intersects at most once. We proceed case by case. We start with the simple cases (1) and (4): since the sandwiched side of β_j is e_1, (as for α_i), both α_i and β_j are made of two sandwiched segments glued along the same side (namely e_1), and hence they intersect at most once. More precisely:

Case (1): Recall that α_i is contained in the parallelogram $P(e_2, e_1)$ and goes from one e_2-side to the opposite side. Let us denote by e, e' the two other sides of $P(e_2, e_1)$. Similarly β_j is contained in another parallelogram $P(e_0, e_1)$ sharing the same diagonal, and β_j goes from one side e_0 to the opposite side. We can see that the intersection of $P(e_2, e_1)$ with $P(e_0, e_1)$ is connected: it is a parallelogram. In particular the intersection of β_j with $P(e_2, e_1)$ goes from the side e to the side e' and thus intersects α_i exactly once (see Figure 6.4).

Case (4): By Remark 6.4 α_i and β_j are contained in the *same* $P(e_2, e_1)$. They both go from one e_2-side to the opposite e_2-side. In particular they intersect at most once.

Next we deal with cases (2), (5) and (6), for which we use the fact that the type of the segment determines a sector for its direction (Remark 6.5).

Case (2): By (6.1), since e_0 is sandwiched by e_1, the direction of β lies in the sector Σ_5. Moreover β_j lies in the parallelogram $P(e_1, e_0)$ and goes from the side e_1 to the opposite (see Figure 6.5). The segments α_i and β_j intersect each other at most twice. Assume by contradiction $\alpha_i \cap \beta_j = \{p, q\}$ with $p \neq q \in X_0$. Since p and q belong to different parts of the segment α_i, they belong to different copies of the $(2m + 1)$-gon. The slope s of the holonomy vector defined by pq coincides with the

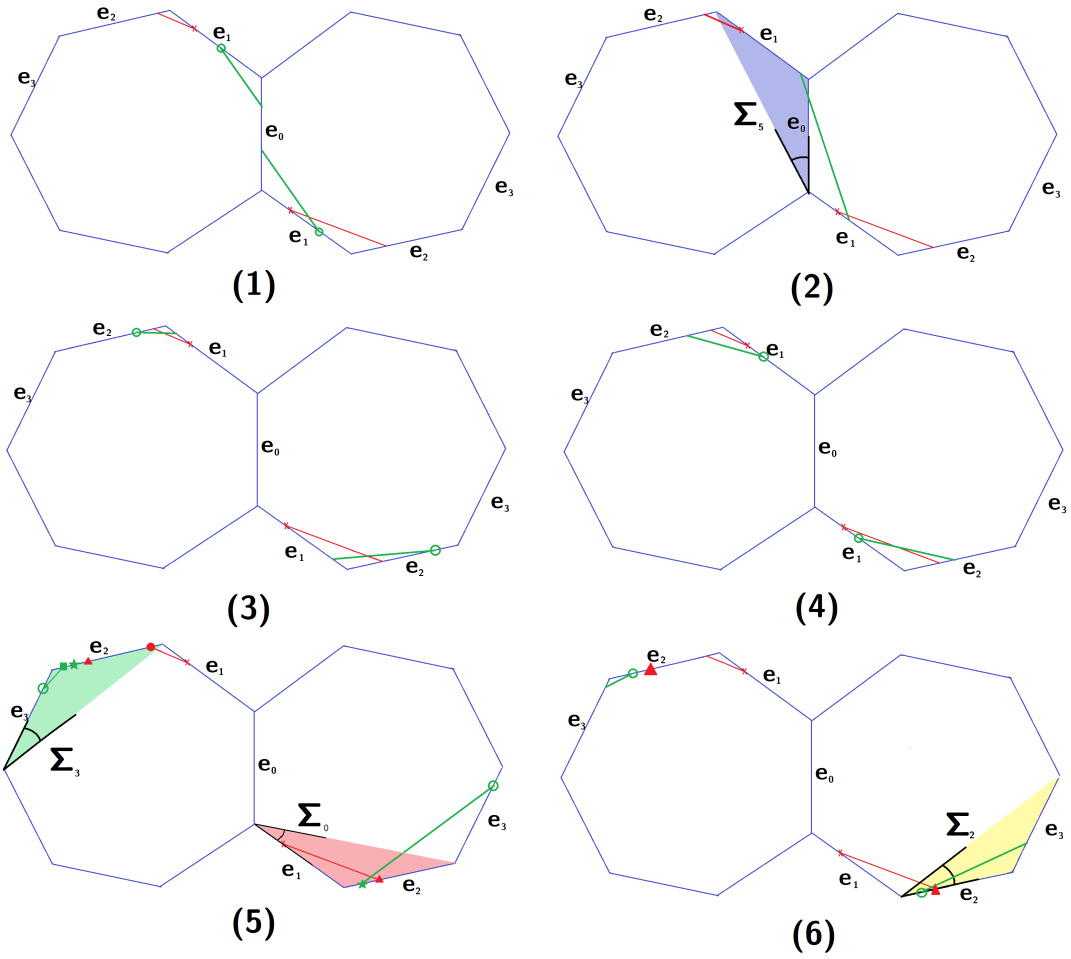

Figure 6.3. The six different cases where α_i (in red) and β_j (in green) are sandwiched and intersect.

slope of β and thus belongs to the sector Σ_5 i.e. $\text{slope}(e_4) \leqslant s \leqslant 0$ (with equality iff β is a diagonal). On the other hand, the intersection of α_i with the two sides e_1 on the plane template of Figure 6.5 determines two points c and d.

By construction the slope s satisfies $s \leqslant \text{slope}(cd)$. Since $\text{slope}(cd) = \text{slope}(e_4)$ we get that β is a diagonal. We run into a contradiction because $\beta_j = \beta$ is not sandwiched (see beginning of Section 6.2), and therefore $\text{Int}(\alpha_i, \beta_j) \leqslant 1$.

Case (6): This case is the same as Case (2) rotating by an angle $\frac{2\pi}{2m+1}$ and swapping α_i and β_j.

Case (5): By (6.1), since e_3 is sandwiched by e_2, the direction of β lies in the sector Σ_3 and β is contained in the parallelogram $P(e_2, e_3)$. In particular its slope verifies $s \geqslant \text{slope}(e_6)$. The segment α_i intersects $P(e_2, e_3)$ with two connected components. One such component intersects one side e_2 at a point a while the other component intersects the other side e_2 at a point b (which project in the double $(2m+1)$-gon to the red bullet and the red triangle in Figure 6.3 Case (5)). As in Case (2) the

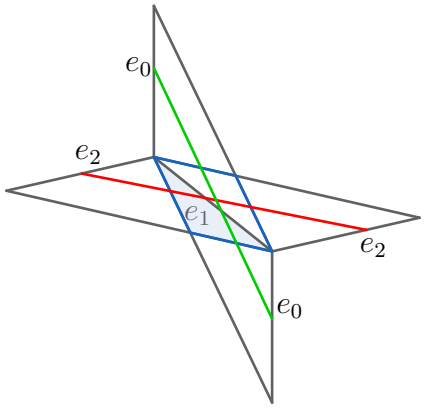

Figure 6.4. Case 1 re-drawn

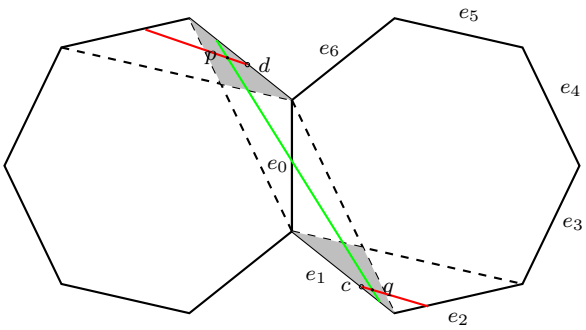

Figure 6.5. The parallelogram $P(e_1, e_0)$ and two intersections in Case (2): $\beta \notin \Sigma_5$

segments α_i and β_j intersect each other at most twice. Assume by contradiction $\alpha_i \cap \beta_j = \{p, q\}$ with $p \neq q \in P(e_2, e_3)$. Necessarily $\text{slope}(ab) \geqslant \text{slope}(pq) = s$. Since $\alpha \in \Sigma_0$ we can check that $\text{slope}(ab) \leqslant \text{slope}(e_6)$ (recall that the slope of α_i' is very close to the slope of α_i).

Thus $s = \text{slope}(e_6)$ and β is a diagonal: we again run into a contradiction because $\beta_j = \beta$ is not sandwiched. Therefore $\text{Int}(\alpha_i, \beta_j) \leqslant 1$ as desired.

Mid-way assessment : at this point let us pause for a second to summarize what we have proved.

Setting aside case (3) which will be considered below, we have for every i, j, $|Int(\alpha_i, \beta_j)| \leqslant 1$. In particular $\sum_{i,j} |Int(\alpha_i, \beta_j)| \leqslant kl$. Recall that we want the quantity on the left to be less than $kl - 1$ instead of kl; the desired bound comes from the following observation: up to permuting α and β, we may assume α is not a diagonal. Then α_1 is non-sandwiched and lies in one of the $(2m+1)$-gons while the second non-sandwiched α_i lies in the other $(2m+1)$-gon[(3)]. In particular, since

[(3)] Notice that the last non-sandwiched segment before a sequence of sandwiched segments and the next non-sandwiched segment after such a sequence lie in different $(2m+1)$-gons, as in Figure 6.7 and Figure 6.8.

β_1 is non sandwiched, it lies in one of the two $(2m+1)$-gons and it cannot intersect both α_1 and the next non-sandwiched α_i.

In particular, $\sum_{i,j} |Int(\alpha_i, \beta_j)| \leqslant kl - 1$. Hence, by Equation (6.2), we get that $Int(\alpha, \beta) \leqslant kl$.

Treating case (3)

In this paragraph we assume there are indices i, j such that α_i is sandwiched of type $e_2 \to e_1 \to e_2$ and β_j is sandwiched of type $e_1 \to e_2 \to e_1$. In this case, α_i and β_j could intersect twice, but we will show that if this happens then there is an index j' such that α_i and $\beta_{j'}$ don't intersect. Hence the conclusion $\sum_{i,j} |Int(\alpha_i, \beta_j)| \leqslant kl$ will still hold (and in fact the inequality will be strict, as we require).

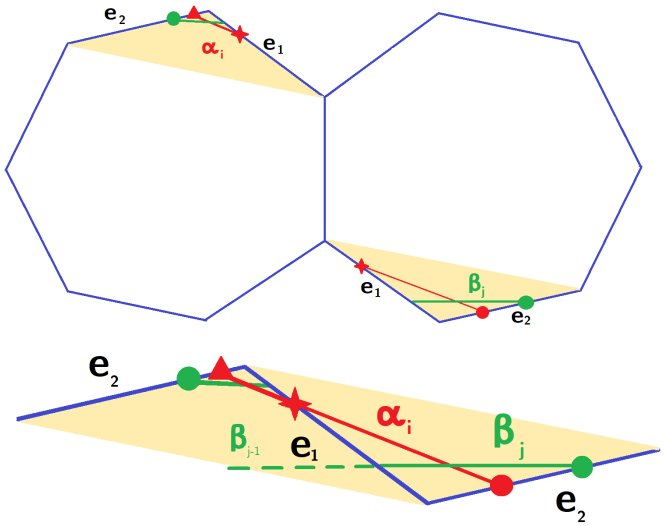

Figure 6.6. α_i and β_j could intersect twice in the configuration of case 3. Below, a closer look at the cylinder $P(e_2, e_1)$. In the example of this picture, α_i does not intersect β_{j-1}.

To do that let us assume $\alpha_{i_0}, \ldots, \alpha_{i_0+p}$ (resp. $\beta_{j_0}, \ldots, \beta_{j_0+q}$) are consecutively sandwiched of type $e_2 \to e_1 \to e_2$ (resp. $e_1 \to e_2 \to e_1$), this sequence being maximal (i.e α_{i_0-1} and α_{i_0+p+1} – resp. β_{j_0-1} and β_{j_0+q+1} – are not sandwiched). An example of such a configuration is depicted in Figure 6.7 for $p = q = 0$ and in Figure 6.8 for $p = q = 3$. We claim that there are at most $(p+3)(q+2)$ intersections between $\alpha_{i_0-1} \cup \alpha_{i_0} \cup \cdots \cup \alpha_{i_0+p} \cup \alpha_{i_0+p+1}$ and $\beta_{j_0-1} \cup \beta_{j_0} \cup \cdots \cup \beta_{j_0+q} \cup \beta_{j_0+q+1}$, while there are $(p+3)(q+3)$ pairs of segments.

Indeed, in this configuration $\alpha_{i_0-1} \cup \alpha_{i_0} \cup \cdots \cup \alpha_{i_0+p} \cup \alpha_{i_0+p+1}$ and $\beta_{j_0-1} \cup \beta_{j_0} \cup \cdots \cup \beta_{j_0+q} \cup \beta_{j_0+q+1}$ go through the cylinder $P(e_2, e_1)$ defined by e_1 and e_2, as in Figure 6.7. Now, instead of cutting β each time it crosses e_1 we can cut β each time it crosses e_2. Notice that β crosses e_1 once more than it crosses e_2, so it gives a decomposition $\beta_{j_0-1} \cup \cdots \cup \beta_{j_0+q} \cup \beta_{j_0+q+1} = \widetilde{\beta}_{j_0} \cup \cdots \cup \widetilde{\beta}_{j_0+q} \cup \widetilde{\beta}_{j_0+q+1}$ with only

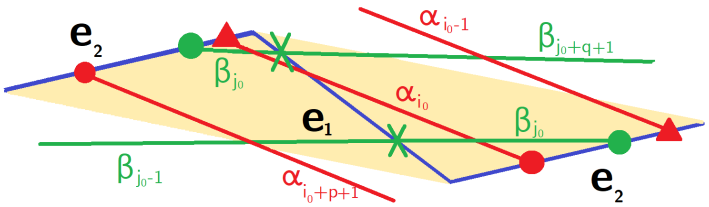

Figure 6.7. $\alpha_{i_0-1} \cup \alpha_{i_0} \cup \cdots \cup \alpha_{i_0+p} \cup \alpha_{i_0+p+1}$ *and* $\beta_{j_0-1} \cup \beta_{j_0-1} \cup \cdots \cup \beta_{j_0+q} \cup \beta_{j_0+q+1}$ *for* $p = q = 0$. *There are only six intersections but nine pairs of segments.*

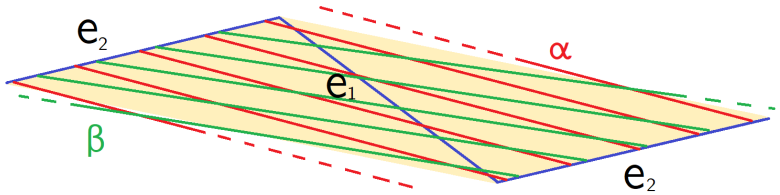

Figure 6.8. $\alpha_{i_0-1} \cup \alpha_{i_0} \cup \cdots \cup \alpha_{i_0+p} \cup \alpha_{i_0+p+1}$ *and* $\beta_{j_0-1} \cup \beta_{j_0} \cup \cdots \cup \beta_{j_0+q} \cup \beta_{j_0+q+1}$ *for* $p = q = 3$. *There are only ten intersections but thirty-six pairs of segments.*

$q+2$ segments while each $\widetilde{\beta}_j$ for $j \in [\![j_0, j_0+q+1]\!]$ can intersect each of the α_i for $i \in [\![i_0-1, i_0+p+1]\!]$ at most once, which leaves at most $(p+3)(q+2)$ intersections.

In conclusion, summing with all other segments yields $\sum_{i,j} |Int(\alpha_i, \beta_j)| < kl$. Adding the possible singular intersection, we get the desired result. This concludes the proof of Lemma 6.8. □

6.4. Conclusion

We are now able to prove the main proposition of this section.

Proof of Proposition 6.1. — If either α or β is not a diagonal, then:

- $l(\alpha)l(\beta) > kl \cdot l_0^2$ by Lemma 6.7,
- $Int(\alpha, \beta) \leqslant kl$ by Lemma 6.8,

In particular, we have:

$$\frac{Int(\alpha, \beta)}{l(\alpha)l(\beta)} < \frac{1}{l_0^2}$$

as desired.

Otherwise, both α and β are diagonals. Then:

(1) either none of them is a side of a $(2m+1)$-gon and then:
   (a) $l(\alpha)l(\beta) \geqslant 4\cos^2(\frac{\pi}{2m+1})l_0^2 > 2l_0^2$ because the shortest diagonals of the $(2m+1)$-gon which are not sides have length $2\cos(\frac{\pi}{2m+1})l_0$.
   (b) $Int(\alpha, \beta) \leqslant 2$ because there is at most one non-singular intersection and one singular intersection.

   In particular, $\frac{Int(\alpha,\beta)}{l(\alpha)l(\beta)} < \frac{1}{l_0^2}$.

(2) or α (up to a change in names) is a side, and then:

(a) $Int(\alpha,\beta) \leqslant 1$ as there is no non-singular intersection,
(b) $l(\alpha)l(\beta) \geqslant l_0^2$ with equality if and only if both α and β are sides of a $(2m+1)$-gon.

In particular, we have $\frac{Int(\alpha,\beta)}{l(\alpha)l(\beta)} \leqslant \frac{1}{l_0^2}$ with equality if and only if both α and β are sides of a $(2m+1)$-gon.

This concludes the proof of Proposition 6.1. □

7. Extension to the Teichmüller disc

In this section, we finally show our main result:

THEOREM 7.1. — *For any surface X in the Teichmüller disc of the double $(2m+1)$-gon, we have:*

$$K(X) = K(0,\infty)\sin\theta(X,0,\infty). \tag{7.1}$$

Theorem 1.1 follows directly as $\sin\theta(X,0,\infty) = \frac{1}{\cosh d_{hyp}(X,\gamma_{0,\infty})}$ by Proposition 4.3. Before proving Theorem 7.1, we show how to deduce Corollary 1.4.

Proof of Corollary 1.4. — Since $\mathrm{Vol}(S_0) = \frac{n}{2}\cos\frac{\pi}{n}$ by Equation (2.2) and the furthest point of $\mathcal{D}$ from $\gamma_{0,\infty}$ is X_0, the corresponding $\sin\theta(X_0,0,\infty)$ being equal to $\sin\frac{\pi}{n}$, Equation (7.1) implies

$$\frac{n}{2}\cos\frac{\pi}{n}\cdot K(0,\infty)\cdot\sin\frac{\pi}{n} \leqslant \mathrm{KVol}(X) \leqslant \frac{n}{2}\cos\frac{\pi}{n}\cdot K(0,\infty).$$

We conclude with Proposition 5.3 and Equation (2.1): $K(0,\infty) = \frac{1}{l(\alpha_m)^2} = \frac{1}{\sin^2\frac{\pi}{n}}$.

The maximum is achieved precisely when $\sin\theta(X,0,\infty) = 1$ i.e. X belongs to the geodesic $\gamma_{0,\infty}$, namely X is the image of S_0 by a diagonal matrix of $\mathrm{SL}(2,\mathbb{R})$. As we have seen the minimum is achieved uniquely at X_0. Finally by Proposition 6.1, the supremum is achieved by pairs of curves that are (images of) pairs of sides of X_0. □

7.1. Interpolation between the regular n-gon and the staircase model

Recall that Proposition 5.1 provides another expression of KVol:

$$K(X) = \sup_{(d,d')} K(d,d')\sin\theta(X,d,d'), \tag{7.2}$$

where the supremum is taken over all pairs (d,d') of distinct periodic directions. The quantity $K(d,d')$ is invariant under the diagonal action of the Veech group. Moreover, we know that Equation (7.1) holds:

- for X in the geodesic $\gamma_{0,\infty}$ by Remark 5.4,
- for $X = X_0$ the double $(2m+1)$-gon by Corollary 6.2.

The main idea of the proof of Theorem 7.1 is to use these two results and interpolate between them to show that Equation (7.1) holds in fact for the whole Teichmüller disc. By symmetry, we can restrict to the surfaces X on the right half of the fundamental

domain, that is on $\mathcal{D}_+ = \{x+iy \mid 0 \leqslant x \leqslant \frac{\Phi}{2} \text{ and } x^2+y^2 \geqslant 1\}$. Using Equation (7.2), it suffices to show that for any pair of distinct periodic directions (d, d') one has:

$$(\clubsuit) \qquad \forall\, X \in \mathcal{D}_+,\ K(d,d')\sin\theta(X,d,d') \leqslant K(0,\infty)\sin\theta(X,0,\infty)$$

The proof is divided in two steps:

(1) Show that it suffices to prove (♣) for $0 \leqslant d < \frac{\Phi}{2} < d'$.
(2) Show that (♣) holds under the assumption $0 \leqslant d < \frac{\Phi}{2} < d'$.

The proof of the first step (Section 7.2) involves hyperbolic geometry and Veech group action, while the second step (Section 7.3) will be deduced from the study of the function

$$X \mapsto \frac{\sin\theta(X,0,\infty)}{\sin\theta(X,d,d')}.$$

7.2. Reduction to convenient geodesics

In this section, we prove that it suffices to verify (♣) for pairs (d, d') with $0 \leqslant d < \frac{\Phi}{2} < d'$. The main step of the proof is Lemma 7.6.

Definition 7.2. — *Given a pair of distinct periodic directions (d, d') and its associated geodesic $\gamma_{d,d'}$ on $\mathbb{H}^2$, we denote by $V(d, d')$ the connected component of $\mathbb{H}^2 \backslash (\Gamma_n.\gamma_{d,d'})$ containing X_0.*

Remark 7.3. — If one of the images of $\gamma_{d,d'}$ by the action of the Veech group Γ_n passes through X_0, then $V(d, d')$ is not well defined. It is convenient, in this case, to set $V(d, d') = \{X_0\}$. Note that in this case there exists $G \in \Gamma_n$ such that $\sin\theta(X_0, G.d, G.d') = 1$, so by Equation (♣) for $X = X_0$ we have

$$\begin{aligned} K(d,d')\sin\theta(X,d,d') &\leqslant K(d,d') = K(G.d,G.d')\sin\theta(X_0,G.d,G.d') \\ &\leqslant K(0,\infty)\sin\theta(X_0,0,\infty) \leqslant K(0,\infty)\sin\theta(X,0,\infty), \end{aligned}$$

therefore, (♣) holds for any $X \in \mathcal{D}_+$.

Remark 7.4. — Notice that, by definition, the boundary of $V(d, d')$ is made of geodesic segments in the Veech group orbit of $\gamma_{d,d'}$. Since d and d' correspond to directions of cusps, there is a finite number of such segments.

Lemma 7.5. — *For any pair of distinct periodic directions (d, d'), the furthest point X_1 from $\gamma_{0,\infty}$ in the boundary of $V(d, d') \cap \mathcal{D}_+$ is further away from $\gamma_{0,\infty}$ than any point $X \in \mathcal{D}_+$ outside $V(d, d')$. Equivalently*

$$\forall\, X \in \mathcal{D}_+ \setminus V(d,d'),\ \sin\theta(X_1,0,\infty) \leqslant \sin\theta(X,0,\infty).$$

Proof. — Take $X \in \mathcal{D}_+ \setminus V(d, d')$ and call g the perpendicular to $\gamma_{0,\infty}$ which contains X. If g intersects $V(d, d')$ then there is an intersection point in the boundary of $V(d, d')$, and this point is further away from $\gamma_{0,\infty}$ than X (see Figure 7.1).

If g does not meet $V(d, d')$, then g intersects the geodesic $\gamma_{\Phi/2,\infty}$ above $V(d, d')$ at M. We claim that the highest point K of

$$V(d,d') \cap \gamma_{\Phi/2,\infty}$$

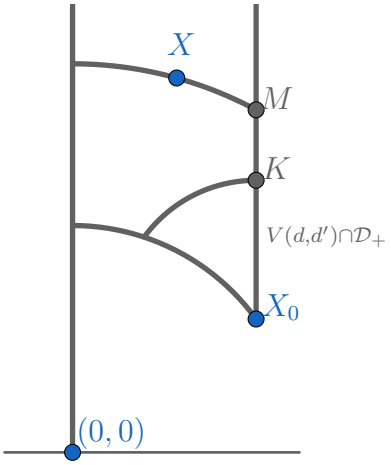

Figure 7.1. The highest K point of $V(d,d')\cap\gamma_{\Phi/2,\infty}$ is further away from $\gamma_{0,\infty}$ than M, which is itself further away from $\gamma_{0,\infty}$ than X.

is further away from $\gamma_{0,\infty}$ than M. Indeed by construction we have the inequality

$$\sin\theta(M,0,\infty)\geqslant\sin\theta(K,0,\infty).$$

By Proposition 4.3, one has $\cosh d_{\mathrm{hyp}}(M,\gamma_{0,\infty})=\sin^{-1}\theta(M,0,\infty)$. Since cosh is an increasing function, we deduce $d_{\mathrm{hyp}}(M,\gamma_{0,\infty})\leqslant d_{\mathrm{hyp}}(K,\gamma_{0,\infty})$. Now since M is by construction further away from $\gamma_{0,\infty}$ than X, this proves the lemma. □

LEMMA 7.6. — *Let (d_1,d_1') and (d_2,d_2') be two pairs of directions such that the associated geodesics $\gamma_{d_1,d_1'}$ and $\gamma_{d_2,d_2'}$ cross the half fundamental domain $\mathcal{D}_+$. We assume that:*

(i) *$K(d_1,d_1')\geqslant K(d_2,d_2')$.*
(ii) *The geodesic $\gamma_{d_2,d_2'}$ lies outside $V(d_1,d_1')$.*
(iii) *(♣) holds for any pair of directions whose associated geodesic is in the boundary of $V(d_1,d_1')$.*

Then (♣) holds for (d_2,d_2').

Proof. — Pick a point $X\in\mathcal{D}_+$. We subdivide the proof in two cases.
First case: $X\notin V(d_1,d_1')$. Then, Lemma 7.5 gives us a point X_1 on the boundary of $V(d_1,d_1')$ such that

$$\sin\theta(X_1,0,\infty)\leqslant\sin\theta(X,0,\infty). \tag{7.3}$$

Note that up to acting by the Veech group, which does not change the conclusion, we may assume that X_1 lies on $\gamma_{d_1,d_1'}$ itself, so $\sin\theta(X_1,d_1,d_1')=1$. Then

$$\begin{aligned}K(d_2,d_2')\sin\theta(X,d_2,d_2') &\leqslant K(d_2,d_2')\\ &\leqslant K(d_1,d_1') \text{ by assumption (i)}\\ &= K(d_1,d_1')\sin\theta(X_1,d_1,d_1') \text{ because } \sin\theta(X_1,d_1,d_1')=1\\ &\leqslant K(0,\infty)\cdot\sin\theta(X_1,0,\infty) \text{ by assumption (iii)}\\ &\leqslant K(0,\infty)\cdot\sin\theta(X,0,\infty) \text{ by (7.3).}\end{aligned}$$

Second case: $X\in V(d_1,d_1')$. Then, by assumption (ii), the perpendicular to $\gamma_{d_2,d_2'}$ through X crosses the boundary of $V(d_1,d_1')$ before it reaches $\gamma_{d_2,d_2'}$, and again, up to acting by the Veech group we may assume the crossing occurs at $\gamma_{d_1,d_1'}$ so that $\sin\theta(X,d_1,d_1')\geqslant\sin\theta(X,d_2,d_2')$. Therefore

$$\begin{aligned}K(d_2,d_2')\sin\theta(X,d_2,d_2') &\leqslant K(d_1,d_1')\sin\theta(X,d_2,d_2') \text{ by assumption (i)}\\ &\leqslant K(d_1,d_1')\sin\theta(X,d_1,d_1')\\ &\leqslant K(0,\infty)\cdot\sin\theta(X,0,\infty) \text{ by assumption (iii),}\end{aligned}$$

which finishes the proof. □

In particular, since we can apply Lemma 7.6 when (d_2,d_2') is in the orbit of (d_1,d_1') under the diagonal action of the Veech group, it suffices to prove (♣) for pairs of directions (d,d') such that some segment of $\gamma_{d,d'}$ is in the boundary of $V(d,d')$. Since $V(d,d')$ is invariant under the dihedral group preserving X_0, it suffices to consider segments of the boundary which are contained in $\mathcal{D}_+$. These geodesics satisfy the following property.

LEMMA 7.7. — *If $\gamma_{d,d'}$ is a geodesic whose closest point to X_0 lies in $\mathcal{D}_+$, then $\gamma_{d,d'}$ intersects the geodesic $\gamma_{\Phi/2,\infty}$. In particular, we can assume $d<\frac{\Phi}{2}<d'$. Moreover, the direction of the tangent vector of $\gamma_{d,d'}$ at the intersection point lies in the first quadrant, in particular $d+d'>\Phi$.*

Proof. — If $\gamma_{d,d'}$ does not intersect the geodesic $\gamma_{\Phi/2,\infty}$, then the perpendicular projection of X_0 to $\gamma_{d,d'}$ lies below X_0, hence not in $\mathcal{D}$, see Figure 7.2 (left part). The statement about the tangent vector at the intersection follows from the convexity of $V(d,d')$ and its symmetry with respect to $\gamma_{\Phi/2,\infty}$. See Figure 7.2 (right part). □

In particular, to prove Theorem 7.1 it suffices to show that (♣) holds for pairs (d,d') with $d<\frac{\Phi}{2}<d'$ and $d+d'>\Phi$. We distinguish two cases:

(1) $d\geqslant 0$
(2) $d<0$

In fact, case 1 is more difficult and will be proven in the next section. However, case 2 can be directly deduced from case 1. Indeed, by Lemma 7.7, if $d<0$ then $d'\geqslant\Phi-d>\Phi$. In particular, $\gamma_{d,d'}$ lies outside $V(0,\Phi)$, whose boundary is made of the geodesic segments that are images of $\gamma_{0,\Phi}$ by the rotation around X_0, in particular $\gamma_{0,\Phi}\cap\mathcal{D}$ is the only boundary of $V(0,\Phi)$ intersecting $\mathcal{D}_+$; see Figure 7.3 for the double pentagon. Since $K(d,d')\leqslant K(0,\Phi)$ (by Proposition 5.3) and the pair

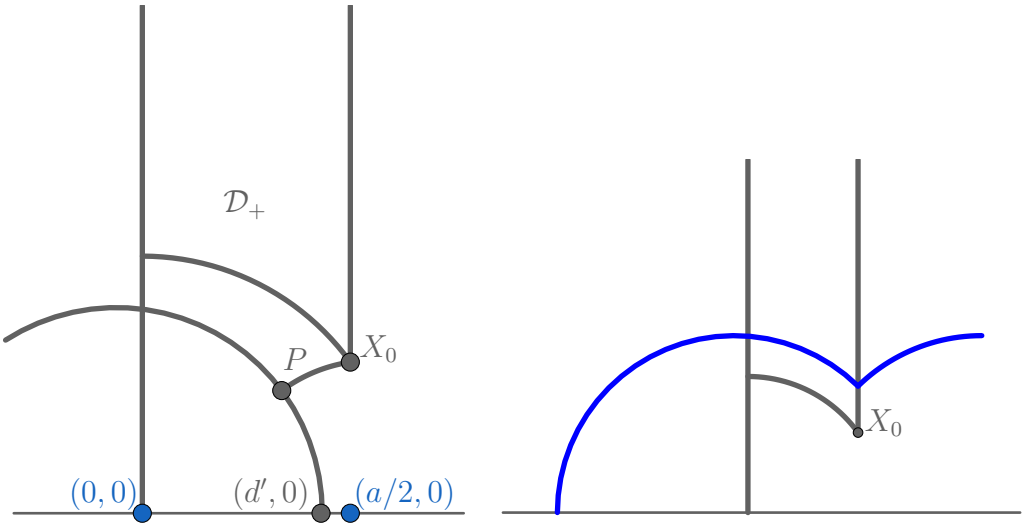

Figure 7.2. Left: when $d' < \Phi/2$, the orthogonal projection of X_0 to $\gamma_{d,d'}$ does not lie in $\mathcal{D}$. Right: when the tangent vector to $\gamma_{d,d'}$ at the intersection with the right boundary of $\mathcal{D}$ does not lie in the first quadrant, $V(X_0, d, d')$ is not convex.

$(0, \Phi)$ satisfies (♣) by case 1, we conclude by Lemma 7.6 that (d, d') satisfies (♣). This shows that case 1 implies case 2.

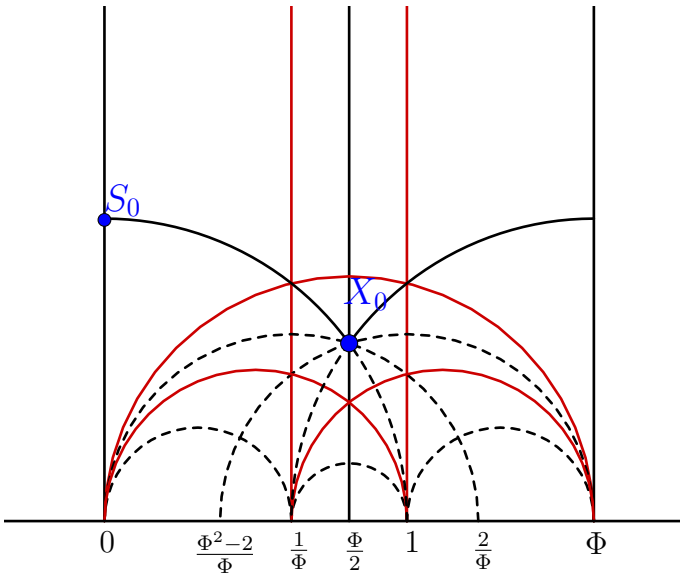

Figure 7.3. The domain $V(0, \Phi)$ for the double pentagon.

7.3. Study of the ratio of sines

In this section we show that any pair of periodic directions (d, d') in case 1 (i.e $0 \leqslant d < \frac{\Phi}{2} < d'$) satisfies (♣). Our proof relies on the study of the function

$$F_{(d,d')} : X \mapsto \frac{\sin\theta(X, 0, \infty)}{\sin\theta(X, d, d')}.$$

More precisely:

PROPOSITION 7.8. — *Under the assumption $0 \leqslant d < \frac{\Phi}{2} < d'$, the function $F_{(d,d')}$ on $\mathcal{D}_+$ takes its minimum at X_0.*

Before giving the proof of this proposition, let us first state and prove the following corollary, which concludes the proof of Theorem 7.1:

COROLLARY 7.9. — *For any (d, d') such that $0 \leqslant d < \frac{\Phi}{2} < d'$, (♣) holds.*

Proof of Corollary 7.9. — Let (d, d') be such that $0 \leqslant d < \frac{\Phi}{2} < d'$, and $X \in \mathcal{D}_+$. We know from Corollary 6.2 that

$$K(d, d')\sin\theta(X_0, d, d') \leqslant K(0, \infty)\sin\theta(X_0, 0, \infty).$$

In particular, by minimality of $F_{(d,d')}$ at X_0

$$K(d, d') \leqslant K(0, \infty)F_{(d,d')}(X_0) \leqslant K(0, \infty)F_{(d,d')}(X)$$

Hence

$$K(d, d')\sin\theta(X, d, d') \leqslant K(0, \infty)\sin\theta(X, 0, \infty)$$

This concludes the proof. □

Proof of Proposition 7.8. — We divide the proof in 5 steps:

(1) We remark that $F_{(d,d')}$ is well defined and differentiable on $\mathbb{H}^2$, and has a well defined minimum on $\mathcal{D}_+$.
(2) We study the gradient of $F_{(d,d')}$ in $\mathcal{D}_+$ and show that it doesn't vanish inside $\mathcal{D}_+$.
(3) We remark that $F_{(d,d')}$ is not minimal at the left boundary of $\mathcal{D}_+$.
(4) We study the variations of $F_{(d,d')}$ on the lower boundary of $\mathcal{D}_+$, which we parametrize as $\left\{(\cos\theta, \sin\theta) : \theta \in \left[\frac{\pi}{n}, \frac{\pi}{2}\right]\right\}$, and show that $F_{(d,d')}$ increases with θ.
(5) We study the variations of $F_{(d,d')}$ on the line $x = \frac{\Phi}{2}$ and show that it increases strictly with y.

Proof of Step 1. — Note that by Proposition 4.3

$$F_{(d,d')}(X) = \frac{\cosh \mathrm{d}_{hyp}(X, \gamma_{d,d'})}{\cosh \mathrm{d}_{hyp}(X, \gamma_{0,\infty})}$$

where $\mathrm{d}_{hyp}(X, \gamma_{d,d'})$ is the hyperbolic distance from X to the geodesic $\gamma_{d,d'}$. Distance functions are not differentiable, but their cosh's are.

Moreover, $F_{(d,d')}(x + iy) \to +\infty$ when $y \to +\infty$ (and $x \in [0, \frac{\Phi}{2}]$), so if $A > 0$ is sufficiently big, we have $F_{(d,d')}(X) > F_{(d,d')}(X_0)$ for any $X = x+iy \in \mathcal{D}_+$ with $y > A$. In particular, $F_{(d,d')}$ reaches its minimum on the compact set $\mathcal{K} = \mathcal{D}_+ \cap \{x+iy | y \leqslant A\}$. This finishes the proof of Step 1.

Proof of Step 2. — Note that since the natural logarithm is an increasing diffeomorphism, we may as well look for the minimum of $\log F_{(d,d')}(X)$ over $\mathcal{D}_+$. Now

$$\begin{aligned}\nabla \log F_{(d,d')}(X) &= \frac{\nabla \cosh \mathrm{d}_{hyp}(X,\gamma_{d,d'})}{\cosh \mathrm{d}_{hyp}(X,\gamma_{d,d'})} - \frac{\nabla \cosh \mathrm{d}_{hyp}(X,\gamma_{0,\infty})}{\cosh \mathrm{d}_{hyp}(X,\gamma_{0,\infty})} \\ &= \tanh \mathrm{d}_{hyp}(X,\gamma_{d,d'})\nabla \mathrm{d}_{hyp}(X,\gamma_{d,d'}) - \tanh \mathrm{d}_{hyp}(X,\gamma_{0,\infty})\nabla \mathrm{d}_{hyp}(X,\gamma_{0,\infty}).\end{aligned}$$

Now the distance gradients are unit vectors, and they are parallel only along the common perpendicular (if it exists) to $\gamma_{0,\infty}$ and $\gamma_{d,d'}$, or never (otherwise), so the gradient of $F_{(d,d')}$ cannot vanish outside of the common perpendicular. Along the common perpendicular, the numbers $\tanh \mathrm{d}_{hyp}(X,\gamma_{d,d'})$ and $\tanh \mathrm{d}_{hyp}(X,\gamma_{0,\infty})$ are equal only at the middle of the common perpendicular segment between the two lines, and there the distance gradients point in opposite directions. So the gradient of $F_{(d,d')}$ cannot vanish at all. Thus $F_{(d,d')}$ does not have a minimum in the interior of $\mathcal{D}_+$.

Proof of Step 3. — On the left boundary of $\mathcal{D}_+$, which is contained in $\gamma_{0,\infty}$, we have $\nabla \mathrm{d}_{hyp}(X,\gamma_{0,\infty}) = 0$, and $\nabla \mathrm{d}_{hyp}(X,\gamma_{d,d'})$ points to the left because $d \geqslant 0$. Therefore no point on the left boundary is a local minimum for $F_{(d,d')}$.

Proof of Step 4. — Now let us study the function $F_{(d,d')}(X)$ restricted to the lower boundary of $\mathcal{D}_+$.

We first give a more convenient expression of $F_{(d,d')}$. Let $X = x + iy$ be a point in the domain $\mathcal{D}_+$. We have

$$\sin\theta(X,0,\infty) = \frac{y}{\sqrt{x^2+y^2}}$$

and since the matrix $\begin{pmatrix} -1 & d \\ \frac{1}{d'-d} & \frac{-d'}{d'-d} \end{pmatrix} \in SL_2(\mathbb{R})$ acts on $\mathbb{H}^2$ by isometry and sends the geodesic $\gamma_{d,d'}$ to $\gamma_{0,\infty}$ and $x+iy$ to

$$\widetilde{x}+i\widetilde{y} = \frac{(-x-iy+d)(d'-d)}{x+iy-d'} = \frac{d-d'}{(x-d')^2+y^2}\cdot(-(x-d)(x-d')-y^2+iy(d'-d))$$

we have:

$$\sin\theta(X,d,d') = \frac{\widetilde{y}}{\sqrt{\widetilde{x}^2+\widetilde{y}^2}} = \frac{y(d'-d)}{\sqrt{((x-d)(x-d')+y^2)^2+y^2(d'-d)^2}}$$

Hence:

$$F_{(d,d')}(X) = \frac{1}{d'-d}\sqrt{\frac{((x-d)(x-d')+y^2)^2+y^2(d'-d)^2}{x^2+y^2}} \tag{7.4}$$

To study the variations of $F_{(d,d')}(X)$, it suffices to consider what is inside the square root in (Equation (7.4)):

$$G : (x,y) \mapsto \frac{((x-d)(x-d')+y^2)^2+y^2(d'-d)^2}{x^2+y^2}$$

On the lower boundary of $\mathcal{D}_+$, this reduces to

$$(1+dd'-(d+d')\cos\theta)^2+(d'-d)^2\sin^2\theta = (1+dd')^2-2(1+dd')(d+d')\cos\theta+2dd'\cos 2\theta-1$$

whose derivative with respect to θ is

$$-4dd'\sin 2\theta + 2(1+dd')(d+d')\sin\theta = 2\sin\theta\left[(1+dd')(d+d') - 4dd'\cos\theta\right].$$

We want to prove that G is an increasing function of θ. This follows from $(1+dd')(d+d') \geqslant 4dd'$, which in turn follows from $d+d' \geqslant 2\sqrt{dd'}$, and the fact that $x^2-2x+1 \geqslant 0$ for any real number x, in particular for $x=\sqrt{dd'}$.

Proof of Step 5. — We compute the differential of G with respect to y. It gives

$$\frac{\partial G}{\partial y}(x,y) = \frac{2y}{(x^2+y^2)^2}\cdot(y^4+2x^2y^2+x^4-dd'(2x-d)(2x-d')).$$

The sign of $\frac{\partial G}{\partial y}(x,y)$ is the sign of the polynomial $P(X) = X^2+2x^2X+x^4-dd'(2x-d)(2x-d')$, which has discriminant

$$\Delta = 4dd'(2x-d)(2x-d').$$

Setting $x=\frac{\Phi}{2}$ yields:

$$\Delta = 4dd'(\Phi-d)(\Phi-d').$$

In particular:

- If $d'>\Phi$, then $\Delta<0$ and P has no real roots.
- If $d'=\Phi$ then $\Delta=0$ and the only real root of P is $-\frac{\Phi^2}{4}<0$.
- Else, $\frac{\Phi}{2}<d'<\Phi$ and P has two real roots:

$$\lambda_- = -\frac{\Phi^2}{4} - \sqrt{dd'(\Phi-d)(\Phi-d')} < 0 \text{ and } \lambda_+ = -\frac{\Phi^2}{4} + \sqrt{dd'(\Phi-d)(\Phi-d')}.$$

But $d(\Phi-d) \leqslant \frac{\Phi^2}{4}$ and $d'(\Phi-d') \leqslant \frac{\Phi^2}{4}$ so $\sqrt{dd'(\Phi-d)(\Phi-d')} \leqslant \frac{\Phi^2}{4}$ and $\lambda_+ \leqslant 0$.

In conclusion, P has no real positive roots, in particular it is positive on $\mathbb{R}_+^*$, and so is $\frac{\partial G}{\partial y}(\frac{\Phi}{2},y)$. This finishes the proof of the last step.

In particular, the only possible minimum for $F_{(d,d')}$ on $\mathcal{D}_+$ is X_0. This proves Proposition 7.8. □

BIBLIOGRAPHY

[Bou22] Julien Boulanger, *Central points of the double heptagon translation surface are not connection points*, Bull. Soc. Math. Fr. **150** (2022), no. 2, 459–472. ↑794

[Bou23a] ———, *Algebraic intersection, lengths and Veech surfaces*, 2023, `https://arxiv.org/abs/2309.17165`. ↑790, 791

[Bou23b] ———, *Quelques problèmes géométriques autour des surfaces de translation*, Ph.D. thesis, Université Grenoble-Alpes, Grenoble, France, 2023. ↑791, 796

[CKM21a] Smail Cheboui, Arezki Kessi, and Daniel Massart, *Algebraic intersection for translation surfaces in a family of Teichmüller disks*, Bull. Soc. Math. Fr. **149** (2021), no. 4, 613–640. ↑788, 789, 791

[CKM21b] ———, *Algebraic intersection for translation surfaces in the stratum $H(2)$*, C. R. Math. **359** (2021), 65–70. ↑788, 789

[DFT11] Diana Davis, Dmitry Fuchs, and Serge Tabachnikov, *Periodic trajectories in the regular pentagon*, Mosc. Math. J. **11** (2011), no. 3, 439–461. ↑794

[DL18] Diana Davis and Samuel Lelievre, *Periodic paths on the pentagon, double pentagon and golden L*, 2018, `https://arxiv.org/abs/1810.11310`. ↑794, 804

[FL23] Sam Freedman and Trent Lucas, *Veech fibrations*, 2023, `https://arxiv.org/abs/2310.02325`. ↑793

[Hoo13] W. Patrick Hooper, *Grid graphs and lattice surfaces*, Int. Math. Res. Not. **2013** (2013), no. 12, 2657–2698. ↑793, 794

[LN14] Erwan Lanneau and Duc-Manh Nguyen, *Teichmüller curves generated by Weierstrass Prym eigenforms in genus 3 and genus 4*, J. Topol. **7** (2014), no. 2, 475–522. ↑791

[Mas96] Daniel Massart, *Normes stables des surfaces*, Ph.D. thesis, École Normale Supérieure de Lyon, 1996. ↑788

[Mas22] ———, *A short introduction to translation surfaces, Veech surfaces, and Teichmüller dynamics*, Surveys in geometry I, Springer, 2022, pp. 343–388. ↑793, 799

[McM05] Curtis T. McMullen, *Teichmüller curves in genus two: Discriminant and spin*, Math. Ann. **333** (2005), no. 1, 87–130. ↑798

[McM07] ———, *Dynamics of $SL_2(\mathbb{R})$ over moduli space in genus two*, Ann. Math. **165** (2007), no. 2, 397–456. ↑798

[MM14] Daniel Massart and Bjoern Muetzel, *On the intersection form of surfaces*, Manuscr. Math. **143** (2014), no. 1-2, 19–49. ↑788, 789, 790

[Mon05] Thierry Monteil, *On the finite blocking property*, Ann. Inst. Fourier **55** (2005), no. 4, 1195–1217. ↑793, 794

[SU10] John Smillie and Corinna Ulcigrai, *Geodesic flow on the Teichmüller disk of the regular octagon cutting sequences and octagon continued fractions maps*, Dynamical numbers. Interplay between dynamical systems and number theory. A special program, May 1–July 31, 2009. International conference, MPI, Bonn, Germany, July 20–24, 2009. Proceedings, Contemporary Mathematics, vol. 532, American Mathematical Society, 2010, pp. 29–65. ↑804

[SU11] ———, *Beyond Sturmian sequences: coding linear trajectories in the regular octagon*, Proc. Lond. Math. Soc. **102** (2011), no. 2, 291–340. ↑804

[SW10] John Smillie and Barak Weiss, *Characterizations of lattice surfaces*, Invent. Math. **180** (2010), no. 3, 535–557. ↑798

[Vee89] William A. Veech, *Teichmüller curves in moduli space, Eisenstein series and an application to triangular billiards*, Invent. Math. **97** (1989), no. 3, 553–583. ↑788, 790, 791, 793, 794, 795

[Vor96] Ya. B. Vorobets, *Planar structures and billiards in rational polygons*, Russ. Math. Surv. **51** (1996), no. 1, 177–178. ↑798

[Wri16] Alex Wright, *From rational billiards to dynamics on moduli spaces*, Bull. Am. Math. Soc. **53** (2016), no. 1, 41–56. ↑793

[Zor06] Anton Zorich, *Flat surfaces*, Frontiers in number theory, physics, and geometry. I On random matrices, zeta functions, and dynamical systems, Springer, 2006, pp. 437–583. ↑793

Manuscript received on 6th January 2023,
revised on 30th March 2024,
accepted on 28th May 2024.

Recommended by Editors X. Caruso and S. Gouëzel.

eISSN: 2644-9463
This journal is a member of Centre Mersenne.

Julien BOULANGER
Institut Fourier, UMR CNRS 5582,
Université Grenoble Alpes,
100, rue des Maths,
38610 Gières (France)
julien.boulanger@univ-grenoble-alpes.fr

Erwan LANNEAU
Institut Fourier,UMR CNRS 5582,
Université Grenoble Alpes,
100, rue des Maths,
38610 Gières (France)
erwan.lanneau@univ-grenoble-alpes.fr

Daniel MASSART
Institut Montpelliérain
Alexander Grothendieck,
CNRS, Univ. Montpellier (France)
daniel.massart@umontpellier.fr